UNIVERSITY OF OKLAHOMA

GRADUATE COLLEGE

Topics on the Scalar Casimir Effect

A Dissertation

Submitted to the Graduate Faculty

in partial fullfillment of the requirements for the

degree of

Doctor of Philosophy

By

JEFFREY ALLEN WAGNER
Norman, Oklahoma
2010

Topics on the Scalar Casimir Effect

A Dissertation Approved for the
Homer L. Dodge Department of Physics and Astronomy

By

Kimball A. Milton, Chair

Howie Baer

Pat Skubic

Eddie Baron

Christian Remling

Acknowledgments

I would like to thank my wife for her love and support during my time as a graduate student at the University of Oklahoma (OU).

I would like to thank the research group at OU, during whose meetings most of the work presented in this dissertation was originally worked out: Kim Milton, my adviser and leader of the research group; Inés Cavero-Pelaez, former student who is now at Zaragoza University in Spain; K. V. Shajesh, another former student who is now a postdoc at Rutgers University in Newark, New Jersey; Prachi Parasha a current student at the OU; Archana Anandakrishnan, a former OU student who transferred to Ohio State University; Elom Abalo a current student of at OU; and Nima Pourtolami another current student at OU.

I would like to thank my colleagues at other institutions whose collaborations has in some way influence the work in this dissertation: Klaus Kirsten, at Baylor University; Stephen Fulling, at Texas A & M University; Martin Schaden, at Rutgers University; Iver Brevik, at the Norwegian University of Science and Technology; and Simen Ellingsen, also at the Norwegian University of Science and Technology.

I would like to acknowledge the National Science Foundation and the Department of Energy for their grants that have supported this research. I would also like to acknowledge the University of Oklahoma and Texas A & M University for their financial support.

Contents

List of Figures

Abstract

Recently the Casimir effect has been getting more popular because of its importance in designing micro and nano scale machines. Working in the language of quantum field theory simplified formulas for the Casimir energy for a massless scalar field are worked out. These formulas are applied to planar potentials and potentials in the annular region between two co-axial cylinders. A scalar equivalent to the Lifshitz formula is applied to new cases of non-trivial planar potentials, specifically two interacting linear potentials and two interacting quadratic potentials. In addition many exact expressions for the Casimir energy between two weakly coupled objects are worked out for many non-trivial geometries. Exact closed form results are shown for parallel cylinders, spheres, and finite ribbons and plates. These closed form results are used to check the range of validity of the proximity force approximation.

Chapter 1

Introduction

The Casimir force refers to the force experienced by two neutral objects due to quantum fluctuations. This force was first noted by the Dutch physicist H. B. G. Casimir in a seminal 1948 paper[1]. However, to explain the Casimir effect it is perhaps best to follow the history. This introduction will start slightly earlier, beginning with London dispersion forces.

1.1 Brief History and Literature Review

In a series of papers in 1930[2, 3, 4] Fritz London described the attraction between two neutral noble gas atoms. The attraction was caused by the instantaneous electric dipole moment of one atom, caused by quantum fluctuations, inducing a dipole moment in the other. Using second order perturbation theory he showed that this instantaneous dipole-induced dipole interaction gave rise to a $1/R^6$ potential. This potential applies for very short separations, because the calculation simply uses the Coulomb potential not accounting for the finite speed of light.

In a 1948 Casimir and Polder[5] calculated the same attraction for two neutral atoms, properly accounting for the finite speed of light by using a retarded potential. Using 4th order perturbation theory they calculated that two neutral atoms which are far away from each other will give rise to a $1/R^7$ potential.

In a second 1948 paper[1] Casimir switched views, no longer thinking about a fluctuating atom interacting through the classical electromagnetic field, but now thinking about the

fluctuating electromagnetic field interacting with extended objects that interact through the imposition of boundary conditions on the electromagnetic field. In this paper Casimir examined perfectly conducting (PC) boundary conditions on two parallel planes a distance a apart. If we switch views like this we have switched now from quantum mechanics to quantum field theory, and this switch introduces some subtleties. Most notable is that the calculated energy in the vacuum state is divergent. However, it turns out that the difference between the vacuum energies for two separations a_1 and a_2 is finite. As a result there is a finite pressure between two parallel perfectly conducting mirrors given by

$$\frac{F}{A} = -\frac{\hbar c \pi^2}{240} \frac{1}{a^4}. \tag{1.1}$$

It should be noted that, even though this is a purely quantum force it is not a exceedingly small force. A quick calculation shows that for two mirrors each 1mm $\times$ 1mm separated by a distance of 1μm would experience a force of about 1.3nN. This force is several orders of magnitude greater than what is now capable of being measured.

The original 1948 result of Casimir was greatly generalized in 1955 by E. M. Lifshitz[6]. He derived a formula to calculate the Casimir pressure between two semi-infinite slabs of dielectric material at any temperature. The materials are simply described by their permittivity $\epsilon(\omega)$, which allows the formula to describe both metals and dielectrics, including in the proper limit Casimir's result for perfect conductors (1.1). The system was generalized even further in 1961 by I. E. Dzyaloshinskii, L. P. Pitaevskii, and Lifshitz to allow a third dielectric to fill the space between the semi-infinite slabs instead of simply vacuum[7]. The derivation of the Lifshitz formula proceeded by looking at the fluctuations in the electric and magnetic currents in the media, not the fluctuations of the electromagnetic field, which

is more reminiscent of the London and Casimir-Polder calculations.

We now have several results showing a force between uncharged objects due solely to quantum fluctuations. This is the Casimir effect.[1] We now have a definition the Casimir effect; however we have two different viewpoints: The sources (i.e. the atom or the dielectric slab) are fluctuating, or the electromagnetic field is fluctuating. The question of which viewpoint was correct was put to rest by J. Schwinger when he showed both formulations, that of a fluctuating source or a fluctuating field, to be equivalent in a 1975 paper[8].

1.2 History and Literature Review of Geometry Dependence of the Casimir Effect

1.2.1 Slab Geometries or Self Stresses

In 1948 Casimir had shown that two perfectly conducting mirrors attracted each other. That led him to propose a model for the electron as a perfectly conducting charged spherical shell, where the electrostatic repulsion is balanced by a Casimir attraction. Unfortunately for the model, a calculation by T. H. Boyer in 1968[9] showed that the pressure on a perfectly conducting shell due to the vacuum energy of the electromagnetic field was positive, directing the shell outward. This outward pressure was opposite to what Casimir had expected, invalidating his model as well as demonstrating an intriguing geometry dependence of the Casimir effect.

In 1979 K. A. Milton[10] calculated the surface stress for a dielectric ball, finding non-

[1] I have lumped all these forces together, whether it is the retarded or non-retarded limits, or whether it is between atom-atom, atom-wall, or two plates. These interactions are often referred to by different names in the literature. In the non-retarded limit, these forces are referred to as van der Waals forces. In the retarded limit atom-atom and atom-wall forces are often referred to as Casimir-Polder forces. Finally the forces dealing only with extended objects are referred to as Casimir forces.

vanishing divergent parts, which muddied the interpretation of the finite part. In 1981 L. L. DeRaad and Milton[11] calculated the pressure for a perfectly conducting infinite cylinder: the pressure turned out to be negative, directing the shell inward. In 1983 Milton[12] and Johnson[13] calculated the Casimir pressure for a spinor field in a spherical shell, this time finding a repulsive result similar to Boyer, although much smaller.[2]

To summarize the results for PC boundary conditions, two parallel plates are attractive, a cylinder is attractive and a sphere is repulsive. It is conceivable that the dimensionality of the surface might have something to do with the sign of the pressure. There have been three papers looking at the Casimir pressure of a scalar field as function of dimensionality of the space-time. The first by J. Ambjørn and S. Wolfram[14] examines a hypercube in D-dimensional spacetime. From this result one could show that parallel plates are attractive for all positive dimensions, only changing sign when continued into negative dimension $D < 1$. The second and third papers by C. Bender and K. A. Milton[15] and K. A. Milton[16] looks at hyperspheres for scalar with Dirichlet and vector fields with perfectly conducting boundary conditions respectively. These papers show two changes of sign of the pressure for the TE mode at every even positive spatial dimension, and a change in sign for the TM mode at $D = 2.6$. The paper shows a finite positive value at $D = 3$, thus reproducing the Boyer result for E&M fields and showing the same sign as Milton's earlier result for spinor fields.

[2] This result has relevance for the bag model for nucleons.

1.2.2 Casimir Effect with Less Symmetric Bodies

All of the previously mentioned results were for systems of very high symmetry. However most experimental systems will not have such perfect symmetries, so we need some results for some more general geometries.

The first attempt at finding the Casimir energy or force between two curved surfaces is known as the proximity force approximation (PFA). The approximation (also known as the Derjaguin approximation) was developed in 1934 by Derjaguin[17] to approximate the force between curved surfaces when only the pressure between planar surfaces was known. It is shown that in the limit when the two surfaces touch the PFA approaches the exact result; this is known as the proximity force theorem. The advantage of the PFA is that it can easily be applied at finite temperature and with real materials, because all that is required is the knowledge of the pressure as a function of separation distance for parallel plates (this is known through the Lifshitz formula). A major disadvantage of the PFA is that the size of the correction term is unknown, and so the range of validity of the PFA is often unknown. There is a more complete explanation of the PFA in appendix C on page 75 with an example calculation, and many results.

The different methods for exploring the Casimir effect often come about by starting the problem in a certain mathematical formalism. One method is to look at the Casimir energy when formulated as a quantum mechanical path integral. One can imagine a situation when the Casimir energy might be dominated by classical paths. In 1998 M. Schaden and L. Spruch exploited this feature and proposed a semi-classical method for evaluating Casimir effects[18]. Using this method, the Casimir energy was represented by a sum over classical periodic paths which dominate the sum over all paths. In 2003 another

semi-classical approach was proposed by R. L. Jaffe and A. Scardicchio called the optical approximation[19, 20, 21]. The optical approximation would include more paths, both periodic and non-periodic, than the simple semi-classical approach. Not leaving out any paths at all, in 2003 H. Gies, K. Langfeld, and L. Moyaerts used the worldline method to numerically calculate Casimir energies[22]. The worldline method works by numerically calculating a path integral using a Monte-Carlo technique. The worldline method is however limited to massless scalar fields with Dirichlet boundary conditions in order for the method to be efficient.

We can explore another set of results by switching mathematical formalism again, to the multiple scattering techniques. In 1971 Renne used such a technique to re-derive the Lifshitz formula from a microscopic point of view[23]. In two papers in 1977 and 1978 R. Balian and B. Duplantier [24, 25] showed that the free energy of the vacuum was finite for a smooth closed perfectly conducting surface. This was shown by formulating the free energy as a convergent sum in a multiple scattering expansion. Some of the critical results are T. Emig for corrugated plates[26], A. Bulgac, P. Magierski, and A. Wirzba for two Dirichlet spheres[27], Emig, Jaffe, Kardar, and Scardicchio for cylinder and a plane[28]. Each of these results is in terms of an expansion, from which by truncating one can make numerical calculations. There have been many other results, which will be discussed further in section 6.

The multiple scattering methods can give quickly converging numerical results, but each new calculation requires major rewriting of the code. Recently, there have been a few papers which use standard engineering numerical electromagnetic methods to calculate the Casimir energies or forces. Recent papers by Johnson *et al* [29, 30, 31] use finite

difference methods, which although not the most efficient, are very general and should work for various systems. More recently Reid *et al*[32] used finite boundary element methods to more efficiently calculate interactions between arbitrary 3-D objects.

1.3 Experimental Status of the Casimir Effect

The experimental history of the Casimir effect is largely a more recent one, because earlier experiments were plagued with many difficulties that often made the experimental error as large or larger than the effects that were being measured. Some of the experimental difficulties included: keeping parallel plates properly aligned, eliminating (or at least characterizing) the electrostatic charges on the surface, reducing and characterizing the surface roughness, keeping the surfaces clean of other contaminants, and accurately measuring the surface separation. Reported below are some of the experiments with conducting metallic surfaces, closest to Casimir's original configuration.

The first attempted measurement was performed in 1958 by M. J. Sparnaay[33]. He performed the experiment with two parallel metal plates and found evidence of a long range force which was consistent with the Casimir force. However due to several experimental difficulties the uncertainty of his measurements of the force were around 100%. In 1972 Sabisky and Anderson[34] verified the Lifshitz formula for dielectrics by using the an experiment with liquid helium thin films, showing excellent agreement between theory and experiment. In 1978 Blokland and Overbeek[35] undertook an experiment with the attraction between a chromium coated plane and a lens. The first modern accurate experiment was performed in 1997 by Lamoreaux[36], who use a torsional balance to measure the force between a gold coated plane and a gold coated spherical lens. He reported measurements

with as little as 5% error, and showed good agreement with Lifshitz theory. However, various systematic effects were not included. Soon after, there were a series of experiments that used an atomic force microscope to measure the force between a gold coated sphere and a gold coated plane[37, 38]. These experiments reported results with enough accuracy that theoretical calculations had to take into account the finite thickness of gold. Recently the most precise measurements were by R. Decca *et al*[39, 40, 41, 42, 43] using a micromechanical oscillator. The measurements are reported to be so precise, such that we can now put limits on forms of non-Newtonian gravity at short distance.

It should be noted that most of the recent experimental results have caused some controversy in the theoretical community. The experimental results obtained at room temperature seem to fit better with a plasma model of the metals instead of a Drude model. However only the Drude model seems to be consistent with the properties of real metals. This dissertation does not deal with this aspect of the Casimir effect. For a thorough discussion on both sides of the thermal issue see Brevik *et al* [44] and Bezerra *et al* [45] and references therein.

1.4 Review Articles

This has been a very brief, and incomplete literature review of the Casimir effect. There have been several recent review articles, including very good articles by Milton [46] and Bordag *et al*[47]. In addition there are several books dedicated to the Casimir effect, including Milton's 2001 monograph[48], and a recent thorough review of the state of Casimir research by Bordag *et al*[49], focused mostly on the experimental situation.

Chapter 2

Mathematical Formalism

This dissertation deals almost exclusively with the scalar Casimir effect. The physical Casimir effect that is measured in experiments is the electromagnetic Casimir effect, and is due to the fluctuating electromagnetic field interacting with objects with electromagnetic properties. An example is the gold sphere and gold plane that is used in R. Decca's experiment. The scalar Casimir effect is due to a fluctuating scalar field, interacting with objects that impose conditions on the scalar field. An example here is imposing Dirichlet boundary conditions for the scalar field on the surface of a sphere.

The scalar Casimir effect is only a toy model which is much easier to study than the full electromagnetic Casimir effect. This model of course has the same benefits and disadvantages as other toy models. It is much easier to understand, often presenting simple analytic results in various approximations. It is useful as a barometer, for calculations which are too difficult to carry out in the toy model will likely be too difficult in the more complicated complete model as well. The toy model can provide insight into the full model and can often predict the qualitative behavior in new situations. However like other toy models it is often overly simplified and cannot give quanitatively correct numbers, and cannot be used to compare to experiment.

There are however cases where the scalar model can provide more than just qualitative insight. In several geometries including all cylindrical geometries, if we assume perfectly conducting boundary conditions, the electromagnetic field breaks into two scalar modes:

the transverse electric (TE) and transverse magnetic (TM) modes. These modes act as scalar fields and obey Dirichlet and Neumann boundary conditions. Furthermore, in a slab geometry the electromagnetic modes can be separated for all boundary conditions, not just perfectly conducting boundary conditions. In these cases studying the scalar fields can give the E&M Casimir effect.

2.1 Notation and Conventions

From this point on in this dissertation, the following conventions will be used. We will work in a set of natural units where Planck's constant ($\hbar$) and the speed of light in a vacuum (c) are set to one,

$$\hbar = c = k = 1. \tag{2.1}$$

We will work entirely in flat space-time, an we will use the "democratic" metric,

$$g_{\mu\nu} = \text{diag}(-1, 1, 1, 1). \tag{2.2}$$

Furthermore we will use the notation given in the following table throughout the dissertation.

Green's Functions	
$3{+}1D$	$\widetilde{G}(x,x')$
$3D$	$G(\vec{x},\vec{x}')$
$2D$	$\mathcal{G}(x_\perp,x'_\perp)$
$1D$	$g(x,x')$
Fourier Variables	
frequency	ω
rotated frequency	ζ
wavenumber or wavevector	k or $k_\perp$,$\vec{k}$
combined wavenumber	$\kappa=\sqrt{\zeta^2+k^2}$

2.2 Scalar Fields

The Lagrangian density of a massless scalar field in a background described by a potential $V(x)$ is given as

$$\mathcal{L}=-\frac{1}{2}\big(\partial\phi(x)\big)^2-\frac{1}{2}V(x)\phi^2(x). \tag{2.3}$$

The action, a functional of the field ϕ and the potential V, is simply the integral over the Lagrangian density,

$$W[\phi,V]=\int \mathrm{d}^4x\mathcal{L}. \tag{2.4}$$

The system must be stationary with respect to infinitesimal changes of the action, $\delta W=0$. By varying the fields we get the equations of motion,

$$\partial_\mu\left(\frac{\partial\mathcal{L}}{\partial(\partial_\mu\phi)}\right)-\frac{\partial\mathcal{L}}{\partial\phi}=0 \quad\longrightarrow\quad \big(-\partial^2+V(x)\big)\phi(x)=0. \tag{2.5}$$

From Noether's theorem we know that if the action remains invariant under an infinitesimal transformation, then there will be a conserved current. For small space-time displacements we will define the stress-energy tensor t^{μ}_{ν},

$$\delta W = \int \mathrm{d}^4 x t^{\mu}_{\nu} \partial_{\mu} \delta x^{\nu}. \tag{2.6}$$

Noether's theorem gives the expression for the conserved stress-energy tensor as

$$t^{\mu}_{\nu} = -\frac{\partial \mathcal{L}}{\partial(\partial_{\mu}\phi)} \partial_{\nu}\phi + \delta^{\mu}_{\nu}\mathcal{L} - \xi\big(\partial^{\mu}\partial_{\nu} - \delta^{\mu}_{\nu}\partial^2\big)\phi^2, \tag{2.7}$$

where the final term that multiplies ξ is a divergence-less term that is bi-linear in the fields. ξ is a constant known as the conformal parameter. For our scalar fields the explicit form of the stress-energy tensor is

$$t_{\mu\nu} = \partial_{\mu}\phi\partial_{\nu}\phi - \frac{1}{2} g_{\mu\nu}\big((\partial\phi)^2 + V\phi^2\big) - \xi\big(\partial_{\mu}\partial_{\nu} - g_{\mu\nu}\partial^2\big)\phi^2. \tag{2.8}$$

The Hamiltonian H is given as the spatial integral of t^{00}. This expression can be simplified by integration by parts, and using the equation of motion (2.5)

$$\begin{aligned} H &= \int \mathrm{d}^3 x\, t^{00}(x) \\ &= \frac{1}{2}\int \mathrm{d}^3 x \Big(\partial_0\phi\partial_0\phi + \nabla\phi\nabla\phi + V\phi^2\Big) + \text{surface terms} \\ &= \frac{1}{2}\int \mathrm{d}^3 x \Big(\partial_0\phi\partial_0\phi + \phi(-\nabla^2 + V)\phi\Big) + \text{s.t.} \\ &= \frac{1}{2}\int \mathrm{d}^3 x \Big(\partial_0\phi\partial_0\phi + \phi(-\partial_0^2)\phi\Big) + \text{s.t.} \end{aligned} \tag{2.9}$$

2.3 Quantized Fields

To examine the Casimir effect we will want to calculate the forces and energy for the vacuum state. To do so we will start with the quantum partition function for a scalar field with a

source $K(x)$,

$$\langle 0_+|0_-\rangle^K = Z[K] = \int \mathcal{D}\phi e^{iW[\phi,V,K]}, \tag{2.10}$$

where the action is the same as (2.4) with a source term added in,

$$W[\phi,V,K] = \int \mathrm{d}^4x\big(\mathcal{L} + K(x)\phi(x)\big). \tag{2.11}$$

We can identify the vacuum expectation value (VEV) for a time ordered product of fields by taking functional derivatives of the partition function with respect to the sources. To calculate the stress-energy tensor or the Hamiltonian we will need the VEV of the product of two fields,

$$\big\langle 0_+|\mathrm{T}\big(\phi(x)\phi(x')\big)|0_-\big\rangle = \frac{1}{Z[0]}\left(i\frac{\delta}{\delta K(x)}\right)\left(i\frac{\delta}{\delta K(x')}\right) Z[K]\Big|_{K\to 0}. \tag{2.12}$$

This expression can be very easily calculated if we rewrite the field as

$$\phi'(x) = \phi(x) - \int \mathrm{d}^4x'\widetilde{G}(x,x')K(x'), \tag{2.13}$$

where $\widetilde{G}$ is the Green's function for the field equations of motion,

$$\big(-\partial^2 + V(x)\big)\widetilde{G}(x,x') = \delta^4(x-x'). \tag{2.14}$$

The action is then written as

$$W[\phi,V,K] = W[\phi',V,0] + \frac{1}{2}\int \mathrm{d}^4x\mathrm{d}^4x' K(x)\widetilde{G}(x,x')K(x'). \tag{2.15}$$

With this we simply identify the time ordered product of fields with the Green's function,

$$\big\langle 0_+|\mathrm{T}(\phi(x)\phi(x'))|0_-\big\rangle = -i\widetilde{G}(x,x'). \tag{2.16}$$

Now it should be noted that the fields would in this case satisfy the expected commutation relation,

$$\big[\phi(x),\dot{\phi}(x')\big]_{t=t'} = i\delta^3(\vec{x}-\vec{x}'). \tag{2.17}$$

It would also be helpful to us to calculate the total energy of the system without having to calculate the local energy density. To do that we will work in the language of the functional determinant. We will define the functional determinant of an operator $\hat{D}$ as

$$\det \hat{D} = \int \mathcal{D}\phi e^{i\int \mathrm{d}^4x \phi \hat{D}\phi}. \tag{2.18}$$

We will use the identity,

$$\det \hat{D} = e^{\ln\det(\hat{D})} = e^{-\operatorname{Tr}\ln(\hat{D}^{-1})}. \tag{2.19}$$

Now, we will integrate by parts in the action from 2.4 to get

$$\begin{aligned} W[\phi, V] &= -\frac{1}{2}\int \mathrm{d}^4x\, \phi(x)\big(-\partial^2 + V(x)\big)\phi(x) \\ &= -\frac{1}{2}\int \mathrm{d}^4x\, \phi(x)\widetilde{G}^{-1}\phi(x). \end{aligned} \tag{2.20}$$

Physically $Z[K=0] = \langle 0_+|0_-\rangle$ is the amplitude of the vacuum evolving from $t=-\infty$ to $t=+\infty$. If we don't have have a potential we are going to say that the vacuum state is stable, so $Z[K=0, V=0] = 1$. Taking these conditions together we can now write, for a general potential $V(x)$,

$$Z[K=0, V] = e^{\frac{1}{2}\operatorname{Tr}\ln \widetilde{G}\widetilde{G}_0^{-1}}. \tag{2.21}$$

Notice that we have completely integrated out the fields, so we can now identify the action as

$$W = -\frac{i}{2}\operatorname{Tr}\ln \widetilde{G}\widetilde{G}_0^{-1}. \tag{2.22}$$

2.4 Casimir Energy Formulas

This dissertation works almost completely in the Green's function method. All the physical properties are calculated from the Green's functions of the systems we're looking at. It is

useful here to collect together all of the formulas which can be used when calculating the Green's function.

By combining equations (2.8) and (2.16) we can now write the VEV of the stress-energy tensor in terms of the Green's function,

$$t_{\mu\nu}(x) = \frac{1}{i}\Big(\partial_\mu\partial'_\nu - \frac{g_{\mu\nu}}{2}\big(\partial^\lambda\partial'_\lambda + V\big)\Big)\widetilde{G}(x,x') \,\Big|_{x'\to x} - \xi\big(\partial_\mu\partial_\nu - g_{\mu\nu}\partial^2\big)\widetilde{G}(x,x). \tag{2.23}$$

In most situations we will be examining time-independent situations, or at least situations which change adiabatically. If that is the case, we can get more useful expressions using the time Fourier transform of the Green's function,

$$\widetilde{G}(x,x') = \int_{-\infty}^{\infty} \frac{\mathrm{d}\omega}{2\pi} e^{-i\omega(t-t')} G(\vec{x},\vec{x}'). \tag{2.24}$$

The energy density is calculated as,

$$u(x) = t^{00} = -\frac{i}{4\pi}\int_{-\infty}^{\infty} \mathrm{d}\omega \bigg(\big(\omega^2 + \nabla\nabla' + V\big)G(\vec{x},\vec{x}') \,\Big|_{\vec{x}'\to\vec{x}} - \xi\nabla^2 G(\vec{x},\vec{x})\bigg). \tag{2.25}$$

Also in a time-independent system, the Hamiltonian is the energy of the system. Working from (2.9) we can then write the energy as

$$E = -\frac{i}{4\pi}\int_{-\infty}^{\infty} \mathrm{d}\omega\; 2\omega^2 \,\mathrm{Tr}(G - G_0), \tag{2.26}$$

where we have subtracted off the energy without any potential at all. Finally we can in a time-independent situation identify the action and the energy by

$$\big\langle 0_+|e^{iW}|0_-\big\rangle = \big\langle 0_+|e^{-iE\tau}|0_-\big\rangle\,, \tag{2.27}$$

where τ is an infinite time constant $\tau = \int \mathrm{d}t$. The energy then becomes

$$E = \frac{i}{2\tau}\,\mathrm{Tr}\ln\widetilde{G}\widetilde{G}_0^{-1}, \tag{2.28}$$

or using the Fourier transform

$$E = \frac{i}{4\pi} \int_{-\infty}^{\infty} \mathrm{d}\omega \, \mathrm{Tr} \ln G G_0^{-1} \tag{2.29}$$

2.5 Multiple Scattering Formula

In Casimir physics we are often interested in the interaction of two bodies. We can rework our expressions for the energy such that it is zero if either individual body is not present; we can subtract out the self energies of both bodies. This procedure has the advantage that, if the two potentials are not overlapping, then the expression is completely finite, and no regularization is needed.

To start we write the Green's function in terms of the free Green's function,

$$G(\vec{x}, \vec{x}') = \big(1 + G_0 V\big)^{-1} G_0. \tag{2.30}$$

Substituting this into equation (2.29) gives

$$E = -\frac{i}{4\pi} \int_{-\infty}^{\infty} \mathrm{d}\omega \, \mathrm{Tr} \ln(1 + G_0 V). \tag{2.31}$$

Let the potential be made up of two separate bodies, $V(\vec{x}) = V_1(\vec{x}) + V_2(\vec{x})$. We can now formally show

$$1 + G_0 V = \big(1 + G_0 V_1\big)\big(1 - V_1(1 + G_0 V_1)^{-1} G_0 V_2 (1 + G_0 V_2)^{-1} G_0\big)\big(1 + G_0 V_2\big). \tag{2.32}$$

We can see, since the expression in equation (2.32) is inside a log, we can clearly separate out the energies due solely to potential V_1 and potential V_2. Defining the interaction energy

as $E_{\rm int} = E_{V_1+V_2} - E_{V_1} - E_{V_2}$ we can derive the formulas

$$E = -\frac{i}{4\pi}\int_{-\infty}^{\infty} \mathrm{d}\omega\, \mathrm{Tr}\ln(1 - T_1 G_0 T_2 G_0), \tag{2.33a}$$

$$E = -\frac{i}{4\pi}\int_{-\infty}^{\infty} \mathrm{d}\omega\, \mathrm{Tr}\ln(1 - V_1 G_1 V_2 G_2). \tag{2.33b}$$

T_i is defined as $T_i = V_i(1 + G_0 V_i)^{-1}$, and is related to the scattering matrix $S_i = 1 - T_i$. G_i is the Green's function that satisfies the equations of motion for a single potential V_i. A much more rigorous derivation of these formula is given by Kenneth and Klich [50].

2.6 Euclidean Rotation

We will often employ a Euclidean rotation, in order to switch the Green's functions from oscillatory functions to exponentially dying functions. The Euclidean rotation is accomplished by rotating the frequency integral from the real to the imaginary axis in a counter-clockwise manner. This has the effect of replacing the frequency ω with the imaginary frequency $i\zeta$.

Using equations (2.25) (2.26), and (2.33b) we get the following useful formulas:

- Energy Density,

$$u(x) = \frac{1}{4\pi}\int_{-\infty}^{\infty} \mathrm{d}\zeta \bigg(\big(-\zeta^2 + \nabla\nabla' + V\big) G(\vec{x}, \vec{x}') \,\Big|_{\vec{x}'\to\vec{x}}\, -\xi\nabla^2 G(\vec{x}, \vec{x}) \bigg), \tag{2.34}$$

- Energy,

$$E = -\frac{1}{4\pi}\int_{-\infty}^{\infty} \mathrm{d}\zeta\, 2\zeta^2\, \mathrm{Tr}(G - G_0), \tag{2.35}$$

- Interaction Energy,

$$E = \frac{1}{4\pi}\int_{-\infty}^{\infty} \mathrm{d}\zeta\, \mathrm{Tr}\ln(1 - V_1 G_1 V_2 G_2). \tag{2.36}$$

Chapter 3

Separation of Variables: the Stäckel Determinant

We are going to define a reduced Green's function by performing a general separation of variables using the Stäckel determinant. We will follow the notation of Morse and Feshbach[51].

We will work in terms of a set of coordinates ξ_i, where $i = 1, 2, 3$. The scale factors h_i are defined in the usual way for orthogonal coordinates, by partial derivatives with respect to Cartesian coordinates.

$$h_i = \sqrt{\left(\frac{\partial \xi_i}{\partial x}\right)^2 + \left(\frac{\partial \xi_i}{\partial y}\right)^2 + \left(\frac{\partial \xi_i}{\partial z}\right)^2}. \tag{3.1}$$

We will perform the separation using the properties of the Stäckel determinant. The Stäckel determinant S is formed from the determinant of the Φ matrix,

$$S = \det \begin{pmatrix} \Phi_{11}(\xi_1) & \Phi_{12}(\xi_1) & \Phi_{13}(\xi_1) \\ \Phi_{21}(\xi_2) & \Phi_{22}(\xi_2) & \Phi_{23}(\xi_2) \\ \Phi_{31}(\xi_3) & \Phi_{32}(\xi_3) & \Phi_{33}(\xi_3) \end{pmatrix}. \tag{3.2}$$

The $i^{\text{th}}, j^{\text{th}}$ component of the Φ matrix, given as $\Phi_{ij}(\xi_i)$, is a function of the single variable ξ_i. The $\Phi_{ij}(\xi_i)$ functions are not unique for a given set of coordinates; however one can find sets of acceptable functions in Morse and Feshbach [51] and Moon and Spencer [52]. The set of coordinates will be separable if the Jacobian of the coordinates is equal to the Stäckel determinant times a product of functions of a single variable,

$$h_1 h_2 h_3 = S f_1(\xi_1) f_2(\xi_2) f_3(\xi_3). \tag{3.3}$$

This equation gives the first relation between the scale factors h_i and the single variable functions used in the separated equations $f_i(\xi_i)$. The f_i functions are also given in references

[51, 52] for all separable coordinate systems. The M_i functions are defined from the minors of the Φ_{ij} matrix,

$$M_i = \det(\text{minor}_{1,i}(\Phi_{ij})) = \frac{\partial S}{\partial \Phi_{i1}} = \frac{S}{h_i^2}. \tag{3.4}$$

Notice that M_i is a function of the two coordinates $\xi_{j\neq i}$, i.e. $M_1(\xi_2, \xi_3)$. These also give the second relation between the scale factors h_i and the functions used in the separation of variables M_i. The minors satisfy the following conditions,

$$\sum_{i=1,2,3} \frac{M_i}{S}\Phi_{1i} = 1, \quad \text{and} \quad \sum_{i=1,2,3} \frac{M_i}{S}\Phi_{ji} = 0. \quad \text{for } j = 2, 3. \tag{3.5}$$

Using this notation the Laplacian can be written as

$$\nabla^2 = \sum_{i=1,2,3} \frac{1}{h_1 h_2 h_3} \frac{\partial}{\partial \xi_i} \frac{h_1 h_2 h_3}{h_i^2} \frac{\partial}{\partial \xi_i} = \sum_{i=1,2,3} \frac{M_i}{S} \frac{1}{f_i} \frac{\partial}{\partial \xi_i} f_i \frac{\partial}{\partial \xi_i}. \tag{3.6}$$

We will assume that the potential has the form

$$V(\vec{x}) = \frac{v(\xi_1)}{h_1^2} = \frac{M_1}{S} v(\xi_1), \tag{3.7}$$

where v depends only on the single variable ξ_1. The delta function can be written as

$$\delta^3(\vec{x} - \vec{x}') = \frac{\delta(\xi_1 - \xi_1')\delta(\xi_2 - \xi_2')\delta(\xi_3 - \xi_3')}{h_1 h_2 h_3} = \frac{\delta(\xi_1 - \xi_1')\delta(\xi_2 - \xi_2')\delta(\xi_3 - \xi_3')}{S f_1 f_2 f_3}. \tag{3.8}$$

The Helmholtz Green's function equation now becomes

$$\begin{aligned} \frac{1}{S}\Bigg[& M_1 \left(-\frac{1}{f_1}\frac{\partial}{\partial \xi_1} f_1 \frac{\partial}{\partial \xi_1} + \Phi_{11}\zeta^2 + \Phi_{12}\alpha_2^2 + \Phi_{13}\alpha_3^2 + v(\xi_1) \right) \\ & + M_2 \left(-\frac{1}{f_2}\frac{\partial}{\partial \xi_2} f_2 \frac{\partial}{\partial \xi_2} + \Phi_{21}\zeta^2 + \Phi_{22}\alpha_2^2 + \Phi_{23}\alpha_3^2 \right) \\ & + M_3 \left(-\frac{1}{f_3}\frac{\partial}{\partial \xi_3} f_3 \frac{\partial}{\partial \xi_3} + \Phi_{31}\zeta^2 + \Phi_{32}\alpha_2^2 + \Phi_{33}\alpha_3^2 \right) \Bigg] G(\vec{x}, \vec{x}') \\ & = \frac{\delta(\xi_1 - \xi_1')\delta(\xi_2 - \xi_2')\delta(\xi_3 - \xi_3')}{S f_1 f_2 f_3}. \end{aligned} \tag{3.9}$$

We write the Green's function as a sum of eigenfunctions times a reduced Green's function,

$$G(\vec{x},\vec{x}') = \sum_{\alpha_2}\sum_{\alpha_3} B(\xi_2',\xi_3')\chi_2(\xi_2)\chi_3(\xi_3)g(\xi_1,\xi_1'). \tag{3.10}$$

The $\chi_2(\xi_2)$ and $\chi_3(\xi_3)$ and α_2 and α_3 are the eigenfunctions and eigenvalues determined by the simultaneous set of equations,

$$\left(-\frac{1}{f_2}\frac{\partial}{\partial\xi_2}f_2\frac{\partial}{\partial\xi_2} + \Phi_{21}\zeta^2 + \Phi_{22}\alpha_2^2 + \Phi_{23}\alpha_3^2\right)\chi_2(\xi_2;\zeta,\alpha_2,\alpha_3) = 0, \tag{3.11a}$$

$$\left(-\frac{1}{f_3}\frac{\partial}{\partial\xi_3}f_3\frac{\partial}{\partial\xi_3} + \Phi_{31}\zeta^2 + \Phi_{32}\alpha_2^2 + \Phi_{33}\alpha_3^2\right)\chi_3(\xi_3;\zeta,\alpha_2,\alpha_3) = 0, \tag{3.11b}$$

along with appropriate boundary conditions. Using this substitution we get

$$\begin{aligned} M_1\sum_{\alpha_2}\sum_{\alpha_3} & B(\xi_2',\xi_3')\chi_2(\xi_2)\chi_3(\xi_3) \\ & \times\left(-\frac{1}{f_1}\frac{\partial}{\partial\xi_1}f_1\frac{\partial}{\partial\xi_1}\Phi_{11}\zeta^2 + \Phi_{12}\alpha_2^2 + \Phi_{13}\alpha_3^2 + v(\xi_1)\right)g(\xi_1,\xi_1') \\ & = \frac{\delta(\xi_2-\xi_2')\delta(\xi_3-\xi_3')}{f_2f_3}\frac{\delta(\xi_1-\xi_1')}{f_1} \end{aligned} \tag{3.12}$$

The χ eigenfunctions are orthogonal with respect to some weighting function $\rho(\xi_2,\xi_3)$,[1]

$$\begin{aligned} \int \mathrm{d}\xi_2\mathrm{d}\xi_3\rho(\xi_2,\xi_3) & \chi_2(\xi_2;\zeta,\alpha_2,\alpha_3)\chi_2(\xi_2;\zeta,\alpha_2',\alpha_3') \\ & \times\chi_3(\xi_3;\zeta,\alpha_2,\alpha_3)\chi_3(\xi_3;\zeta,\alpha_2',\alpha_3') = \delta_{\alpha_2,\alpha_2'}\delta_{\alpha_3,\alpha_3'}. \end{aligned} \tag{3.13}$$

Plugging everything in together and taking advantage of the orthogonality condition, we can conclude that

$$B(\xi_2,\xi_3) = \frac{\rho(\xi_2,\xi_3)}{M_1(\xi_2,\xi_3)f_2(\xi_2)f_3(\xi_3)}\chi_2(\xi_2)\chi_3(\xi_3), \tag{3.14}$$

which lets us write the full Green's function as

$$G(\vec{x},\vec{x}') = \frac{\rho(\xi_2,\xi_3)}{M_1(\xi_2,\xi_3)f_2(\xi_2)f_3(\xi_3)}\sum_{\alpha_2,\alpha_3}\chi_2(\xi_2)\chi_2(\xi_2')\chi_3(\xi_3)\chi_3(\xi_3')g(\xi_1,\xi_1'). \tag{3.15}$$

[1] Here the χ functions are chosen to be real, but the form can easily be adjusted to allow for complex functions.

The reduced Green's function g satisfies the reduced Green's function equation,

$$\left(-\frac{1}{f_1}\frac{\partial}{\partial\xi_1}f_1\frac{\partial}{\partial\xi_1}+\Phi_{11}\zeta^2+\Phi_{12}\alpha_2^2+\Phi_{13}\alpha_3^2+v(\xi_1)\right)g(\xi_1,\xi_1';\zeta,\alpha_2,\alpha_3)=\frac{\delta(\xi_1-\xi_1')}{f_i}. \tag{3.16}$$

3.1 Interaction Casimir Energy with a Separable Potential

Working with the interaction Casimir energy written with the multiple scattering formula given by equation (2.36), by expanding the log we can write

$$E=-\frac{1}{4\pi}\int_{-\infty}^{\infty}\mathrm{d}\zeta\sum_{s=1}^{\infty}\frac{1}{s}\,\mathrm{Tr}(V_1G_1V_2G_2)^s. \tag{3.17}$$

The trace can be written as

$$\mathrm{Tr}(V_1G_1V_2G_2)^s=\int\mathrm{d}^3x_1\mathrm{d}^3x_1'\cdots\mathrm{d}^3x_s'V_1(\vec{x}_1)G_1(\vec{x}_1,\vec{x}_1')\cdots V_2(\vec{x}_s')G_2(\vec{x}_s',\vec{x}_1). \tag{3.18}$$

We can now substitute equations (3.3) (3.7) and (3.15) into the trace. The Sf_2f_3 term from the Jacobian, and the M_1/S from the potential perfectly combine to allow us to use the orthogonality condition shown in equation (3.13). This leaves us with

$$\begin{aligned}\mathrm{Tr}(V_1G_1V_2G_2)^s&=\sum_{\alpha_2,\alpha_3}\int f_1(\xi_1)\mathrm{d}\xi_1\cdots\mathrm{d}\xi_s'v_1(\xi_1)g_1(\xi_1,\xi_1')\cdots v_2(\xi_s')g_2(\xi_s',\xi_1)\\&=\sum_{\alpha_2,\alpha_3}\mathrm{tr}(g_1v_1g_2v_2)^s.\end{aligned} \tag{3.19}$$

We show in section 4.1.3 that if the potentials v_1 and v_2 are non-overlapping then the resulting Green's function is a product of two functions as shown in equation (4.45). In that case it is trivial to show

$$\mathrm{tr}(v_1g_1v_2g_2)^s=\left(\mathrm{tr}\,v_1g_1v_2g_2\right)^s, \tag{3.20}$$

which allows us to rewrite the interaction Casimir energy as

$$E = \frac{1}{4\pi} \int_{-\infty}^{\infty} \mathrm{d}\zeta \sum_{\alpha_2,\alpha_3} \ln(1 - \operatorname{tr} v_1 g_1 v_2 g_2). \tag{3.21}$$

3.2 Trace of the Green's Function with Separable Coordinates

To obtain the full Casimir energy, which includes self energies, we can work with the ζ^2 trace equation (2.35). The trace of the Green's function is written in separable coordinates as

$$\begin{aligned} \operatorname{Tr}(G - G_0) &= \int (\mathrm{d}^3 x) \Big(G(\vec{x}, \vec{x}) - G_0(\vec{x}, \vec{x}) \Big) \\ &= \sum_{\alpha_2,\alpha_3} \int (S f_1 f_2 f_3 \mathrm{d}\xi_1 \mathrm{d}\xi_2 \mathrm{d}\xi_3) \frac{\rho(\xi_2, \xi_3)}{M_1 f_2 f_3} \chi_2^2(\xi_2) \chi_3^2(\xi_3) \Big(g(\xi_1, \xi_1) - g_0(\xi_1, \xi_1) \Big). \end{aligned} \tag{3.22}$$

For general coordinates we do not know a specific form for $\rho(\xi_2, \xi_3)$, so we must make some further simplifications to move on. The assumption we will make is that we are either working in a cylindrical coordinate system, or a rotationally invariant coordinate system, and the potential is independent of the z or azimuthal coordinate respectively.[2] In either case, assigning the z or ϕ coordinate to ξ_3 we have the conditions,

$$\Phi_{31}(\xi_3) = \Phi_{32}(\xi_3) = 0, \tag{3.23a}$$

which implies,

$$M_1(\xi_2, \xi_3) = \Phi_{22}(\xi_2) \Phi_{33}(\xi_3), \quad \text{and} \quad S = (\Phi_{11}\Phi_{22} - \Phi_{21}\Phi_{12})\, \Phi_{33}. \tag{3.23b}$$

[2] These coordinate systems can or course be treated in a more traditional way. It can be said that using the full Stäckel determinant for these situations is like using a hammer to swat a fly, but we have already bought the hammer, and it's nice to see how it's used for the simpler situation.

Because Φ_{31} and Φ_{32} are zero, the ξ_3 eigenvalue equation,

$$-\frac{1}{f_3}\frac{\partial}{\partial\xi_3}f_3\frac{\partial}{\partial\xi_3}\chi_3(\xi_3;\alpha_3) = -\Phi_{33}\alpha_3^2\chi_3(\xi_3;\alpha_3), \tag{3.24}$$

is independent of ζ and α_2, and will uniquely determine α_3. This Sturm-Liouville type equation will guarantee the existence of orthogonal solutions, which satisfy the eigenvalue condition,

$$\int \mathrm{d}\xi_3\Phi_{33}(\xi_3)f(\xi_3)\chi_3(\xi_3;\alpha_3)\chi_3(\xi_3;\alpha_3') = \delta_{\alpha_3,\alpha_3'}. \tag{3.25}$$

Since the value of α_3 is explicitly set by equation (3.24) we can write the eigenvalue equation for ξ_2 in similar Sturm-Liouville type,

$$\left[-\frac{1}{f_2}\frac{\partial}{\partial\xi_2}f_2\frac{\partial}{\partial\xi_2} + \Phi_{21}\zeta^2 + \Phi_{23}\alpha_3^2\right]\chi_2(\xi_2;\zeta,\alpha_2,\alpha_3) = -\Phi_{22}\alpha_2^2\chi_2(\xi_2;\zeta,\alpha_2,\alpha_3). \tag{3.26}$$

This will give a second orthogonality condition for the second equation

$$\int \mathrm{d}\xi_2\Phi_{22}(\xi_2)f(\xi_2)\chi_2(\xi_2;\zeta,\alpha_2,\alpha_3)\chi_2(\xi_3;\zeta,\alpha_2',\alpha_3) = \delta_{\alpha_2,\alpha_2'}. \tag{3.27}$$

These orthogonality conditions give the explicit form of $\rho(\xi_2,\xi_3)$

$$\rho(\xi_2,\xi_3) = M_1 f_2 f_3. \tag{3.28}$$

Using the orthogonality conditions we can now write

$$\begin{aligned}\mathrm{Tr}(G-G_0) = \sum_{\alpha_3}\sum_{\alpha_2}\Bigg[&\int \mathrm{d}\xi_1\Phi_{11}(\xi_1)f_1(\xi_1)\Big(g(\xi_1,\xi_1)-g_0(\xi_1,\xi_1)\Big)\\ &-\int \mathrm{d}\xi_2\Phi_{21}(\xi_2)f_2(\xi_2)\chi_2^2(\xi_2)\int \mathrm{d}\xi_1\Phi_{12}(\xi_1)f_1(\xi_1)\Big(g(\xi_1,\xi_1)-g_0(\xi_1,\xi_1)\Big)\Bigg].\end{aligned} \tag{3.29}$$

3.2.1 Cylindrical Coordinates, z-invariant Potentials

Suppose the potential is sepearable in a cylindrical coordinate system, which includes circular cylindrical, parabolic cylindrical, hyperbolic cylindrical, and cartisian. For these po-

tentials we will identify $\xi_3 = z$ and $\alpha_3 = k_z$, the momentum wavevector in the z direction. In these simplified coordinates we have the conditions

$$\Phi_{33}(z) = -1, \quad \text{and} \quad f_3(z) = 1, \tag{3.30}$$

for the z component, and

$$\Phi_{11}(\xi_1) = \Phi_{13}(\xi_1) \quad \text{and} \quad \Phi_{21}(\xi_2) = \Phi_{23}(\xi_2), \tag{3.31}$$

for the other two coordinates.

The full Green's function is then written as

$$G(\vec{x}, \vec{x}') = \int_{-\infty}^{\infty} \frac{\mathrm{d}k_z}{2\pi} e^{ik_z(z-z')} \sum_{\alpha_2} \chi_2(\xi_2)\chi_2(\xi_2')g(\xi_1, \xi_1'). \tag{3.32}$$

Making the identification $\zeta^2 + k_z^2 = \kappa^2$, we have the eigenfunction condition in the ξ_2 variable as

$$\left[-\frac{1}{f_2}\frac{\partial}{\partial\xi_2} f_2 \frac{\partial}{\partial\xi_2} + \Phi_{21}\kappa^2\right] \chi_2(\xi_2; \kappa, \alpha_2) = -\Phi_{22}\alpha_2^2 \chi_2(\xi_2; \kappa, \alpha_2). \tag{3.33}$$

The orthogonality condition for ξ_2 is the same, and we can use the identity (A.4) to evaluate the second ξ_2 integral

$$\begin{aligned} &\int \mathrm{d}\xi_2 \Phi_{21}(\xi_2) f_2(\xi_2) \chi_2^2(\xi_2) \\ &\qquad = f_2(\xi_2) \left(\frac{\partial}{\partial\xi_2}\chi_2(\xi_2)\frac{\partial}{\partial\kappa}\chi_2(\xi_2) - \chi_2(\xi_2)\frac{\partial}{\partial\kappa}\frac{\partial}{\partial\xi_2}\chi_2(\xi_2) \right) \Big|_{\xi_2 \to \text{endpoints}} \end{aligned} \tag{3.34}$$

The Casimir energy can now be written as

$$\begin{aligned} E = \frac{L_z}{4\pi} \int_{-\infty}^{\infty} \kappa \mathrm{d}\kappa \sum_{\alpha_2} \Bigg[&\int \mathrm{d}\xi_1 \Phi_{11}(\xi_1) f_1(\xi_1) \Big(g(\xi_1, \xi_1) - g_0(\xi_1, \xi_1) \Big) \\ -f_2(\xi_2) \left(\frac{\partial}{\partial\xi_2}\chi_2(\xi_2)\frac{\partial}{\partial\kappa}\chi_2(\xi_2) - \chi_2(\xi_2)\frac{\partial}{\partial\kappa}\frac{\partial}{\partial\xi_2}\chi_2(\xi_2) \right) \Big|_{\xi_2 \to \text{endpoints}} &\int \mathrm{d}\xi_1 \Phi_{12}(\xi_1) f_1(\xi_1) \Big(g(\xi_1, \xi_1) - g_0(\xi_1, \xi_1) \Big) \Bigg]. \end{aligned} \tag{3.35}$$

3.2.2 Rotational Coordinates, ϕ-invariant Potentials

For azimuthally symmetric coordinate systems we will define $\xi_3 = \phi$, and $\alpha_3 = m$. We have the conditions

$$\Phi_{33}(\phi) = -1, \quad \text{and} \quad f_3(\phi) = 1. \tag{3.36}$$

The full Green's function is written

$$G(\vec{x}, \vec{x}') = \frac{1}{2\pi} \sum_{m=-\infty}^{\infty} e^{im(\phi-\phi')} \sum_{\alpha_2} \chi_2(\xi_2)\chi_2(\xi_2')g(\xi_1, \xi_1'). \tag{3.37}$$

Again, we use identity (A.4) to evaluate the second ξ_2 integral

$$\int \mathrm{d}\xi_2 \Phi_{21}(\xi_2) f_2(\xi_2) \chi_2^2(\xi_2)$$
$$= f_2(\xi_2) \left(\frac{\partial}{\partial \xi_2}\chi_2(\xi_2)\frac{\partial}{\partial \zeta}\chi_2(\xi_2) - \chi_2(\xi_2)\frac{\partial}{\partial \zeta}\frac{\partial}{\partial \xi_2}\chi_2(\xi_2) \right) \Bigg|_{\xi_2 \to \text{endpoints}} \tag{3.38}$$

The Casimir energy can now be written as

$$E = \frac{1}{8\pi^2} \int_{-\infty}^{\infty} \mathrm{d}\zeta \sum_{m=-\infty}^{\infty} \sum_{\alpha_2} \Bigg[\int \mathrm{d}\xi_1 \Phi_{11}(\xi_1) f_1(\xi_1) \Big(g(\xi_1, \xi_1) - g_0(\xi_1, \xi_1) \Big)$$
$$- f_2(\xi_2) \left(\frac{\partial}{\partial \xi_2}\chi_2(\xi_2)\frac{\partial}{\partial \zeta}\chi_2(\xi_2) - \chi_2(\xi_2)\frac{\partial}{\partial \zeta}\frac{\partial}{\partial \xi_2}\chi_2(\xi_2) \right) \Bigg| \int \mathrm{d}\xi_1 \Phi_{12}(\xi_1) f_1(\xi_1) \Big(g(\xi_1, \xi_1) - g_0(\xi_1, \xi_1) \Big) \Bigg]. \tag{3.39}$$
$$\xi_2 \to \text{endpoints}$$

Chapter 4

Green's Functions for Sturm-Liouville Operators

From the separation of variables we will always be left with a reduced Green's function equation for a Sturm-Liouville type operator,

$$\left[-\frac{\partial}{\partial x}p(x)\frac{\partial}{\partial x}+q(x)\right]g(x,x')=\delta(x-x'). \tag{4.1}$$

The $q(x)$ function can be identified from equation (3.16) as

$$q(x)=f_1(x)\big(\zeta^2\Phi_{11}+\alpha_2^2\Phi_{12}(x)+\alpha_3^2\Phi_{13}^1+v(x)\big). \tag{4.2}$$

One method of finding the Green's functions is to start with the homogeneous solution for $x<x'$ and $x>x'$ and then apply matching conditions to $g(x,x')$ at $x=x'$. Let $y=A(x)$ and $y=B(x)$ be two linearly independent solutions to the homogeneous differential equation

$$\left[-\frac{\partial}{\partial x}p(x)\frac{\partial}{\partial x}+q(x)\right]y(x)=0. \tag{4.3}$$

The Green's function can then be written as

$$g^{\pm}(x,x')=\alpha^{\pm}(x')A(x)+\beta^{\pm}(x')B(x), \tag{4.4}$$

where the plus sign is for $x>x'$ and the minus is for $x<x'$. The matching conditions can be derived by integrating the differential equation 4.1, and are explicitly given by

$$\begin{aligned} g^-(x,x')\big|_{x=x'}-g^+(x,x')\big|_{x=x'}&=0\\ \frac{\mathrm{d}}{\mathrm{d}x}g^-(x,x')\bigg|_{x=x'}-\frac{\mathrm{d}}{\mathrm{d}x}g^+(x,x')\bigg|_{x=x'}&=\frac{1}{p(x')}. \end{aligned} \tag{4.5}$$

Substituting the Green's function (4.4) into the matching conditions (4.5) gives the explicit formula,

$$\begin{aligned}(\alpha^-(x') - \alpha^+(x'))A(x') + (\beta^-(x') - \beta^+(x'))B(x') = 0 \\ (\alpha^-(x') - \alpha^+(x'))A'(x') + (\beta^-(x') - \beta^+(x'))B'(x') = \frac{1}{p(x')}.\end{aligned} \tag{4.6}$$

It is now possible to solve for $\alpha^+(x')$ in terms of $\alpha^-(x') = \alpha(x')$ and $\beta^-(x')$ in terms of $\beta^+(x') = \beta(x')$. Doing so gives us the Green's functions

$$\begin{aligned}g^+(x,x') &= \frac{A(x)B(x')}{W[A,B](x')p(x')} + \alpha(x')A(x) + \beta(x')B(x), \\ g^-(x,x') &= \frac{B(x)A(x')}{W[A,B](x')p(x')} + \alpha(x')A(x) + \beta(x')B(x),\end{aligned} \tag{4.7}$$

where $W[A,B](x)$ is the Wronskian $A(x)B'(x) - A'(x)B(x)$. It is well known that the Wronskian times the weight function $p(x)$ is a constant,

$$W[A,B](x)p(x) = C. \tag{4.8}$$

By using this property, we can now write the Green's function as

$$g(x,x) = \frac{1}{C}A(x_>)B(x_<) + \alpha(x')A(x) + \beta(x')B(x), \tag{4.9}$$

where $x_>(x_<)$ is defined as the greater(lesser) of x and x'.

4.1 Green's Functions in Multiple Regions

In most problems the potential will be a piecewise continuous potential given by the expression

$$v(x) = v_i(x) \qquad \text{for } x_i < x < x_{i+1}, \tag{4.10}$$

where the x_i's are the boundaries between the various regions. Explicitly x_i is the boundary between the $(i-1)^{\text{th}}$ and i^{th} region, or stated another way x is in the i^{th} region if $x_i < x < x_{i+1}$. An example potential is shown in figure 4.1.

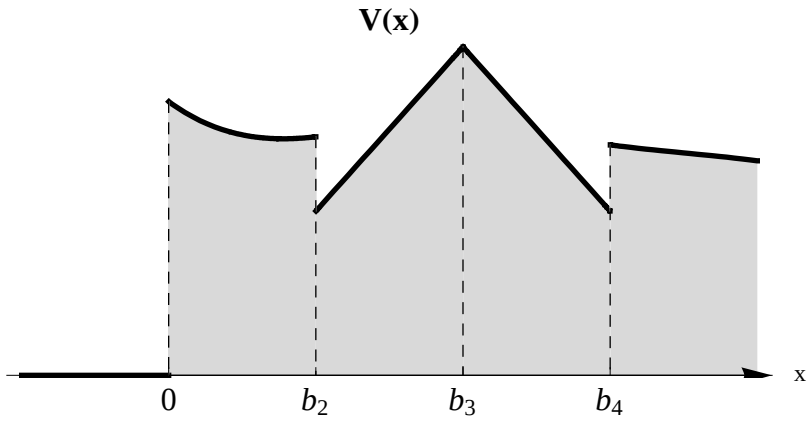

Figure 4.1: This is an example potential for a general potential $v(x)$ that is explicitly given by a piecewise continuous function, where $v(x) = v_i(x)$ in the i^{th} region.

When x is in the i^{th} region and x' is not in the i^{th} region, the Green's function equation (4.1) becomes an homogenous differential equation, because the inhomogeneous term $\delta(x - x') = 0$ when the points cannot coincide. The Green's function would then be given by a general solution to (4.3),

$$g(x, x') = \alpha_i(x')A_i(x) + \beta_i(x')B_i(x), \tag{4.11}$$

where $y = A_i$ and $y = B_i$ are the independent solutions to the equation (4.3) in the i^{th} region.

4.1.1 Region to Region Matching Conditions

If we modify equation (4.9) to include indices i which indicate which region x and x' are located, and combine it with (4.11) we now have the Green's function everywhere with undetermined coefficients α_i's and β_i's. To determine these coefficients we have to apply matching conditions on the boundaries of the regions, and boundary conditions on the edges of the domain of x. The matching conditions between the boundaries can also be derived by integrating equation (4.1). As long as the general potential $v(x)$ is reasonably well behaved[1], i.e.

$$\int_{x_i-\epsilon}^{x_i+\epsilon} \mathrm{d}x V(x) = 0, \tag{4.12}$$

then the matching conditions at the boundary x_i are simply continuity of the Green's function and its derivative,

$$\begin{aligned} g(x,x')\big|_{x=x_i-} - g(x,x')\big|_{x=x_i+} &= 0 \\ \frac{\mathrm{d}}{\mathrm{d}x}g(x,x')\bigg|_{x=x_i-} - \frac{\mathrm{d}}{\mathrm{d}x}g(x,x')\bigg|_{x=x_i+} &= 0. \end{aligned} \tag{4.13}$$

Using equations (4.9) and (4.11) we can rewrite equation (4.13) out explicitly as

$$\begin{aligned} &\alpha_i(x')A_i(x_i) + \beta_i(x')B_i(x_i) - \alpha_{i+1}(x')A_{i+1}(x_i) \\ &\qquad - \beta_{i+1}(x')B_{i+1}(x_i) = \begin{cases} \frac{B_{i+1}(x_i)}{C_{i+1}}A_{i+1}(x') & \text{for } x_i < x' < x_{i+1} \\ -\frac{A_i(x_i)}{C_i}B_i(x') & \text{for } x_{i-1} < x' < x_i \\ 0 & \text{otherwise,} \end{cases} \end{aligned} \tag{4.14a}$$

[1] This condition essentially states that the potential cannot have any Dirac delta functions on the boundaries without changing the matching conditions.

$$\alpha_i(x')A_i'(x_i) + \beta_i(x')B_i'(x_i) - \alpha_{i+1}(x')A_{i+1}'(x_i)$$

$$-\beta_{i+1}(x')B_{i+1}'(x_i) = \begin{cases} \frac{B_{i+1}'(x_i)}{C_{i+1}}A_{i+1}(x') & \text{for } x_i < x' < x_{i+1} \\ -\frac{A_i'(x_i)}{C_i}B_i(x') & \text{for } x_{i-1} < x' < x_i \\ 0 & \text{otherwise.} \end{cases} \tag{4.14b}$$

We can simplify the matching conditions considerably by taking an appropriate linear combination of the equations in the system of equation (4.14). An appropriate choice for the linear combination would be $B_{i+1}'(x_i)$(4.14a)$-B_{i+1}(x_i)$(4.14b), and $A_i'(x_i)$(4.14a)$-A_i(x_i)$(4.14b):

$$W[A_i, B_{i+1}](x_i)\alpha_i(x') + W[B_i, B_{i+1}](x_i)\beta_i(x')$$

$$-W[A_{i+1}, B_{i+1}](x_i)\alpha_{i+1}(x') = \begin{cases} -\frac{W[A_i,B_{i+1}](x_i)}{C_i}B_i(x') & \text{for } x_{i-1} < x' < x_i \\ 0 & \text{otherwise} \end{cases} \tag{4.15a}$$

$$-W[A_i, B_i](x_i)\beta_i(x') + W[A_i, A_{i+1}](x_i)\alpha_{i+1}(x')$$

$$+W[A_i, B_{i+1}](x_i)\beta_{i+1}(x') = \begin{cases} -\frac{W[A_i,B_{i+1}](x_i)}{C_{i+1}}A_{i+1}(x') & \text{for } x_i < x' < x_{i+1} \\ 0 & \text{otherwise.} \end{cases} \tag{4.15b}$$

4.1.2 Boundary Conditions - Forming the Matrix Equation

Now with equation (4.15) we see that we can form a matrix equation for the unknown functions $\alpha_i(x)$ and $\beta_i(x)$. The matrix equation has the form

$$\begin{pmatrix} \ddots & \ddots & & & & & \\ \ddots & \ddots & \ddots & & & & \\ & a_{2i+1} & b_{2i+1} & c_{2i+1} & & & \\ & & a_{2i+2} & b_{2i+2} & c_{2i+2} & & \\ & & & \ddots & \ddots & \ddots & \\ & & & & \ddots & \ddots & \end{pmatrix} \begin{pmatrix} \vdots \\ \alpha_i \\ \beta_i \\ \alpha_{i+1} \\ \beta_{i+1} \\ \vdots \end{pmatrix} = \begin{pmatrix} 0 \\ \vdots \\ 0 \\ -(c_{2j}/C_j)A_j \\ -(a_{2j+1}/C_j)B_j \\ 0 \\ \vdots \\ 0 \end{pmatrix}. \tag{4.16}$$

The coefficients of the matrix a_i b_i and c_i differ depending on whether the index i is even or odd, and are explicitly,

$$\begin{aligned} a_{2i} &= -W[A_{i-1}, B_{i-1}](x_{i-1}) & a_{2i+1} &= W[A_i, B_{i+1}](x_i) \\ b_{2i} &= W[A_{i-1}, A_i](x_{i-1}) & b_{2i+1} &= W[B_i, B_{i+1}](x_i) \\ c_{2i} &= W[A_{i-1}, B_i](x_{i-1}) & c_{2i+1} &= -W[A_{i+1}, B_{i+1}](x_i). \end{aligned} \tag{4.17}$$

The target vector in equation (4.16) depends on the location of x', which we will take to be in the j^{th} region ($x_{j-1} < x' < x_j$). From equation (4.15) we see that the right hand side of the equation is mostly zero with 2 exceptions; where the $i = j - 1$ for equation (4.15b) and $i = j$ for (4.15a).

Now we know how the center of the matrix works, but we would like to know how first and last rows look as well. At this point we have to think a little about the physics of our

problem. If the range of x is non-periodic, and can be either an open or closed interval from x_- to x_+ where x_+ can be positive infinity and x_- can be negative infinity. In this case it is good to consider an $N+1$ region problem with $i = 0, \ldots, N$. There are boundary conditions imposed on $g(x, x')$ at $x = x_+$ and $x = x_-$. The simplest conditions are Dirichlet where $g(x_+, x') = g(x_-, x') = 0$.

Now we will examine the boundary condition at x_-. This boundary is the left edge of region 0. Assume that x' is not in region 0 then the form of the Green's function at the boundary is

$$g(x_-, x') = \alpha_0(x')A_0(x_-) + \beta_0(x')B_0(x_-). \tag{4.18}$$

Here we will make the assumption that the boundary conditions are such that we can set one of the two independent solutions to zero. If x_- is not a singular point we will only consider Robin type boundary conditions where the value of the logarithmic derivative is given at the boundary. Both Dirichlet and Neumann boundary conditions, where the value of the Green's function or its derivative must vanish on the boundary respectively, are the limiting cases of Robin type boundary conditions. If x_- is a singular point we will consider only the solution which remains regular at the endpoint.

Since equation (4.3) is linear, any two independent linear combinations of $A_0(x)$ and $B_0(x)$ is also a valid set of functions. It turns out it is always possible to define the $A_0(x)$ and $B_0(x)$ solutions such that the boundary condition uniquely specifies $\alpha_0(x') = 0$. We chose the solutions as such to simplify the system of equations. Reversing that statement, the boundary condition at x_- restricts the choice of $B_0(x)$.

Taking the condition that $\alpha_0 = 0$, the matching conditions at x_1 would then give

$$\begin{aligned} b_1\beta_0(x') + c_1\alpha_1(x') &= 0 \\ a_2\beta_0(x') + b_2\alpha_1(x') + c_2\beta_1(x') &= 0, \end{aligned} \tag{4.19}$$

assuming x' is in neither region 0 or 1. A similar argument can be supposed at x_+. We can choose $A_N(x)$ such that $\beta_N = 0$ is completely specified by the boundary conditions at x_+. The matching conditions for x_N are then

$$\begin{aligned} a_{2N-1}\alpha_{N-1} + b_{2N-1}\beta_{N-1}(x') + c_{2N-1}\alpha_n(x) &= 0 \\ a_{2N}\beta_{N-1}(x') + b_{2N}\alpha_N(x') &= 0, \end{aligned} \tag{4.20}$$

again assuming x' is in neither region $N-1$ or N.

We can now fully form a square $2N \times 2N$ tri-diagonal matrix equation for the α and β functions,

$$\begin{pmatrix} b_1 & c_1 & & & \\ a_2 & \ddots & \ddots & & \\ & \ddots & \ddots & c_{2N-1} & \\ & & a_{2N} & b_{2N} \end{pmatrix} \begin{pmatrix} \beta_0 \\ \alpha_1 \\ \vdots \\ \alpha_N \end{pmatrix} = \begin{pmatrix} 0 \\ \vdots \\ -\frac{c_{2j}}{C_j}A_j(x') \\ -\frac{a_{2j+1}}{C_j}B_j(x') \\ \vdots \\ 0 \end{pmatrix}. \tag{4.21}$$

4.1.3 Finding the Green's Function

In appendix B we construct the solution to a general $n \times n$ tri-diagonal matrix equation, with arbitrary target vector d_i. The solution takes the form

$$\begin{aligned} x_i = \frac{1}{\det(M_1^n)} \Bigg(& (-1)^i \sum_{j=1}^{i-1} (-1)^j d_j \det(M_1^{j-1}) \det(M_{i+1}^n) \prod_{m=j+1}^{i} a_m \\ & + d_i \det(M_1^{i-1}) \det(M_{i+1}^n) + (-1)^i \sum_{j=i+1}^{n} (-1)^j d_j \det(M_1^{i-1}) \det(M_{j+1}^n) \prod_{m=i}^{j-1} c_m. \Bigg), \end{aligned} \tag{4.22}$$

where M_i^j is the block of the matrix that starts and ends with the i^{th} and j^{th} rows respectively.

We can now apply the general tri-diagonal solution, equation (4.22) to the problem at hand, given in equation (4.21). It should be noted that our problem has at most two nonzero components of the target vector which makes our solution relatively easy to write down.

In the $2N$ dimensional vector of αs and βs, we can see the $\alpha_i(x')$ corresponds to the $2i^{\text{th}}$ row, and $\beta_i(x')$ the $(2i+1)^{\text{th}}$ row. A quick calculation shown that if x' is in the j^{th} region, then for $j < i$, $\alpha_i(x')$ and $\beta_i(x')$ can be written as

$$\alpha_i(x') = \frac{\det(M_{2i+1}^{2N}) \prod_{m=2j+1}^{2i} a_m}{C_j \det(M_1^{2N})} \left(-c_{2j} \det(M_1^{2j-1}) A_j(x') + \det(M_1^{2j}) B_j(x') \right), \tag{4.23}$$

$$\beta_i(x') = \frac{\det(M_{2i+2}^{2N}) \prod_{m=2j+1}^{2i+1} a_m}{C_j \det(M_1^{2N})} \left(c_{2j} \det(M_1^{2j-1}) A_j(x') - \det(M_1^{2j}) B_j(x') \right). \tag{4.24}$$

For $j > i$ we would have

$$\alpha_i(x') = \frac{\det(M_1^{2i-1}) \prod_{m=2i}^{2j} c_m}{C_j \det(M_1^{2N})} \left(- \det(M_{2j+1}^{2N}) A_j(x') + a_{2j+1} \det(M_{2j+2}^{2N}) B_j(x') \right), \tag{4.25}$$

$$\beta_i(x') = \frac{\det(M_1^{2i}) \prod_{m=2i+1}^{2j} c_m}{C_j \det(M_1^{2N})} \left(\det(M_{2j+1}^{2N}) A_j(x') - a_{2j+1} \det(M_{2j+2}^{2N}) B_j(x') \right), \tag{4.26}$$

and finally for $i = j$ we have

$$\begin{aligned} \alpha_i(x') = \frac{1}{C_i \det(M_1^{2N})} \Bigg(& - c_{2i} \det(M_1^{2i-1}) \det(M_{2i+1}^{2N}) A_i(x') \\ & + c_{2i} a_{2i+1} \det(M_1^{2i-1}) \det(M_{2i+2}^{2N}) B_i(x') \Bigg), \end{aligned} \tag{4.27}$$

$$\begin{aligned} \beta_i(x') = \frac{1}{C_i \det(M_1^{2N})} \Bigg(& c_{2i} a_{2i+1} \det(M_1^{2i-1}) \det(M_{2i+2}^{2N}) A_i(x') \\ & - a_{2i+1} \det(M_1^{2i}) \det(M_{2i+2}^{2N}) B_i(x') \Bigg). \end{aligned} \tag{4.28}$$

The solution as it would be written now would only be taking advantage of the tri-diagonal nature of the system of equations, it would not yet take advantage of the fact that the constants are all given by Wronskians of the differential equations, and some simplifications might occur. These two simplifications emerge simply by examination of the

coefficients in equation (4.17). We see that in every set of two rows two of the coefficients are the same,

$$a_{2i-1} = c_{2i}. \tag{4.29}$$

The next simplification comes from the fact that

$$\begin{aligned} -a_{2i} &= W[A_{i-1}, B_{i-1}](x_{i-1}) = \frac{C_{i-1}}{p(x_{i-1})} \\ -c_{2i+1} &= W[A_{i+1}, B_{i+1}](x_i) = \frac{C_{i+1}}{p(x_i)} \end{aligned} \tag{4.30}$$

The last simplification come from an identify for the Wronskian,

$$\begin{aligned} W[A_{i-1}, A_i](x)W[B_{i-1}, B_i](x) - W[A_{i-1}, B_{i-1}](x)W[A_i, B_i](x) \\ = -W[A_{i-1}, B_i](x)W[A_i, B_{i-1}](x). \end{aligned} \tag{4.31}$$

If we adopt the notation that

$$\widetilde{c}_{2i} = W[A_i, B_{i-1}](x_{i-1}), \tag{4.32}$$

we can rewrite equation (4.31) as

$$b_{2i}b_{2i-1} - a_{2i}c_{2i-1} = -\widetilde{c}_{2i}a_{2i-1}. \tag{4.33}$$

We can now use these formula to simplify the tri-diagonal determinants. If we expand the determinant along the bottom row of the matrix we get the recursion relation,

$$\det(M_i^j) = b_j \det(M_i^{j-1}) - a_j c_{j-1} \det(M_i^{j-2}). \tag{4.34}$$

If we apply this recursion relation twice we get the relation,

$$\det(M_i^j) = (b_j b_{j-1} - a_j c_{j-1}) \det(M_i^{j-2}) - b_j a_{j-1} c_{j-2} \det(M_i^{j-3}). \tag{4.35}$$

Using equations (4.33) and (4.29) and the recursion relations (4.34) and (4.35) we prove in appendix B.1 that the tri-diagonal determinants that start with the first row can be written as

$$\det(M_1^{2i}) = \prod_{j=1}^{i}(-a_{2j-1})\Delta_1^{2i} \quad \text{and} \quad \det(M_1^{2i+1}) = \prod_{j=1}^{i}(-a_{2j-1})\Delta_1^{2i+1}, \tag{4.36}$$

where the Δ_1^i are given by a simple recursion relation. The first few Δs are given by,

$$\Delta_1^1 = b_1 \quad \text{and} \quad \Delta_1^2 = \widetilde{c}_2. \tag{4.37}$$

Further terms can be calculated with the recursion relations,

$$\Delta_1^{2i+1} = b_{2i+1}\Delta_1^{2i} + a_{2i+1}\Delta_1^{2i-1}, \tag{4.38}$$

$$\Delta_1^{2i+2} = \widetilde{c}_{2i+2}\Delta_1^{2i} - b_{2i+2}\Delta_1^{2i-1}, \tag{4.39}$$

Similar to the recursion relation involving the Δs we can find a simplification for determinants that end with the $2N^{\text{th}}$ row,

$$\det(M_{2i-1}^{2N}) = \prod_{j=i}^{N}(-a_{2j-1})\Upsilon_{2i-1}^{2N} \quad \text{and} \quad \det(M_{2i-2}^{2N}) = \prod_{j=i}^{N}(-a_{2j-1})\Upsilon_{2i-2}^{2N}. \tag{4.40}$$

The first few terms are given as

$$\Upsilon_{2N}^{2N} = b_{2N} \quad \text{and} \quad \Upsilon_{2N-1}^{2N} = \widetilde{c}_{2N} \tag{4.41}$$

The recursion relations are

$$\Upsilon_{2i-2}^{2N} = b_{2i-2}\Upsilon_{2i-1}^{2N} + c_{2i-2}\Upsilon_{2i}^{2N}, \tag{4.42}$$

$$\Upsilon_{2i-3}^{2N} = \widetilde{c}_{2i-2}\Upsilon_{2i-1}^{2N} - b_{2i-3}\Upsilon_{2i}^{2N}. \tag{4.43}$$

Using these simplifications the αs and βs greatly simplify. For example the first term in equation (4.23) can now be written

$$\frac{\det(M_1^{2j-1})(-c_{2j})\prod_{m=2j+1}^{2i}(a_m)\det(M_{2i+1}^{2N})}{C_j\det(M_1^{2N})} = \frac{\prod_{s=j+1}^{i-1}C_s}{\prod_{s=j}^{i-1}p(x_s)}\frac{\Delta_1^{2j-1}\Upsilon_{2i+1}^{2N}}{\Delta_1^{2N}} \tag{4.44}$$

Using this simplification, for x and x' not in the same region we get

$$g(x,x') = \frac{\prod_{s=j+1}^{i-1} C_s}{\prod_{s=j}^{i-1} p(x_s)\Delta_1^{2N}} \left(\Delta_1^{2j-1} A_j(x_<) + \Delta_1^{2j} B_j(x_<)\right) \left(\Upsilon_{2i+1}^{2N} A_i(x_>) + \Upsilon_{2i+2}^{2N} B_i(x_>)\right) \tag{4.45}$$

and for x and x' in the same region we get

$$g(x,x') = \frac{A_i(x_>)B_i(x_<)}{C_i} + \frac{1}{C_i\Delta_1^{2N}} \left(\Delta_1^{2i-1}\Upsilon_{2i+1}^{2N} A_i(x)A_i(x') + \Delta_1^{2i}\Upsilon_{2i+2}^{2N} B_i(x)B_i(x') \right.$$
$$\left. + \Delta_1^{2i-1}\Upsilon_{2i+2}^{2N}(A_i(x)B_i(x') + B_i(x)A_i(x'))\right). \tag{4.46}$$

Chapter 5

Application of Separation of Variables

In this chapter we will examine two specific applications of the genereal results from the previous two chapters. First we will examine the simpler case of planar geometries in cartisian coordinates. We will reproduce many known results, and some new numerical results as well. Second we will examine the Casimir energy of two delta function potentials in the annular region between two coaxial cylidrical surface, which we have called an annular piston.

5.1 Planar Geometries: Scalar Equivalent of the Lifshitz Formula

First we will consider the simplest case of planar geometries. Our differential equation will be explicitly

$$\left[-\frac{\mathrm{d}^2}{\mathrm{d}z^2}+\kappa^2+v(z)\right]g_\zeta(z,z')=\delta(z-z') \tag{5.1}$$

This is the simplest of the separable coordinates to consider, and we will use it as the first case to study.

Here we will consider the interaction energy of two planar potentials. The potentials will be general potentials as shown in figure 5.1. We will use the equation (3.21), however with Cartesian coordinates the α sums are replaced by integrals over wavevector. In addition there was a $\delta_{\alpha\alpha}$, which gets replace by a delta function evaluated at zero, so $\delta(k_x=0)=L_x/2\pi$. This delta function corresponds physically to the volume in the coordinate. So for

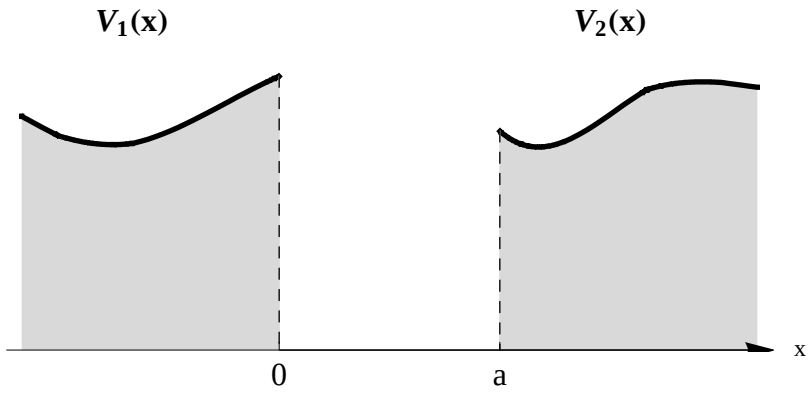

Figure 5.1: Two non-overlapping potentials $v_1(z)$ and $v_2(z)$, separated by a distance a.

a Cartesian coordinate the equation for the interaction energy per unit area $\mathfrak{E}$ in (3.21) becomes

$$\mathfrak{E} = \frac{1}{16\pi^3} \int_{\infty}^{\infty} \mathrm{d}\zeta \int_{\infty}^{\infty} \mathrm{d}k_x \int_{\infty}^{\infty} \mathrm{d}k_y \ln\left(1 - \int \mathrm{d}z\mathrm{d}z' v_1(z) g_1(z,z') v_2(z') g_2(z',z)\right). \tag{5.2}$$

We will treat each potential as a many region potential exactly like that shown in figure 4.1 which is zero for $z < 0$ and becomes nonzero at $z = 0$. In the region where the potential is zero, the solutions to the differential equation are,

$$A_0(z) = e^{-\kappa z} \quad \text{and} \quad B_0(z) = e^{\kappa z}. \tag{5.3}$$

We can then write the Green's function from equation (4.45) as

$$g(z,z') = e^{\kappa z_<} \left[\frac{\prod_{s=1}^{i-1} C_s}{\Delta_1^{2N}} \left(\Upsilon_{2i+1}^{2N} A_i(z_>) + \Upsilon_{2i+2}^{2N} B_i(z_>) \right) \right]. \tag{5.4}$$

Plugging this expression into the z, z' integral inside the logarithm gives us the expression

$$\mathfrak{E} = \frac{1}{4\pi^2} \int_0^{\infty} \kappa^2 \mathrm{d}\kappa \ln\left(1 - \widetilde{R}_1 \widetilde{R}_2 e^{-2\kappa a}\right), \tag{5.5}$$

where the $\widetilde{R}$s are reflection coefficients given by the formula

$$\widetilde{R} = \sum_{i=1}^{N} \left(\frac{\prod_{s=1}^{i-1} C_s}{\Delta_1^{2N}} \right) \int_{z_i}^{z_{i+1}} \mathrm{d}z v_i(z) e^{-\kappa z} \left(\Upsilon_{2i+1}^{2N} A_i(z) + \Upsilon_{2i+2}^{2N} B_i(z) \right). \tag{5.6}$$

This is the scalar equivalent to the Lifshitz formula for dielectrics.

5.1.1 Specific examples

For the case where were the potential only has 2 regions (so N=1) we can greatly simplify the expression for the for reflection coefficient to

$$\widetilde{R} = \frac{1}{\kappa A(0) - A'(0)} \int_0^\infty \mathrm{d}z e^{-\kappa z} A(z), \tag{5.7}$$

where $A(z)$ is the solution to the differential equation in the region where the potential is non-zero which goes to zero at infinity. For a constant potential $v(z) = \sigma$, the reflection coefficient is given by

$$\widetilde{R} = \frac{\sigma}{(\kappa + \kappa')^2} = \frac{\kappa' - \kappa}{\kappa' + \kappa}, \tag{5.8}$$

where $\kappa'^2 = \kappa^2 + \sigma$. This is equivalent to (and written identically to) the well known expression for the TE reflection coefficient between a dielectric surface and vacuum. With this expression we can take the limit as $\sigma \to \infty$, where the potential becomes perfectly reflecting, or $\widetilde{R} \to 1$. In that case the Casimir energy per unit area evaluates to the well known value

$$\mathfrak{E} = -\frac{\pi^2}{1440} \frac{1}{a^3}. \tag{5.9}$$

In addition to constant potentials we can write the reflection coefficients for any system where we can explicitly solve the differential equation. Two examples are linear potentials $v(z) = mz$ with the solution as Airy functions, and quadratic potentials $v(z) = cz^2$ with

the solution as parabolic cylinder functions. The Casimir energies for these configurations are shown in figures 5.2(a) and 5.2(b) respectively.

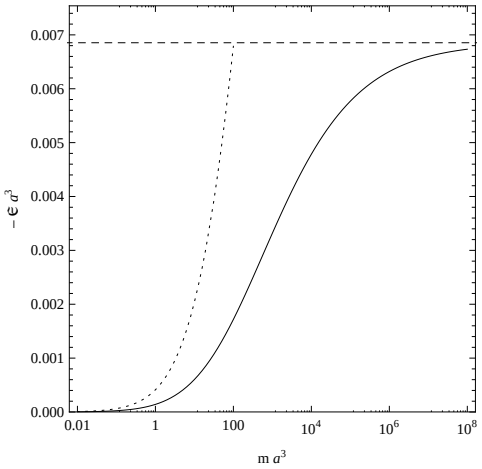

(a) A plot of Casimir energy per unit area scaled by a^3 vs. the unitless parameter ma^3 between two linear potentials $v(z) = mz$. The solid line is the exact soluiton. The dotted line uses a WKB approximation to the differential equation.

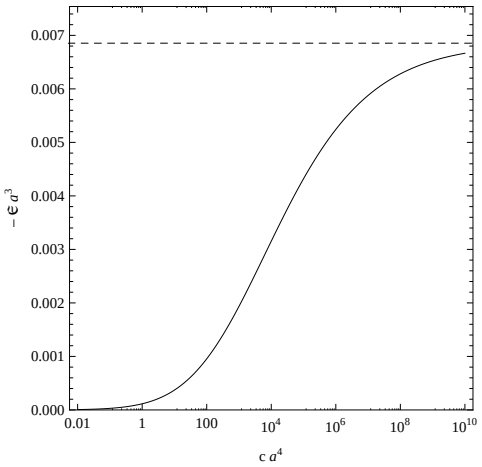

(b) A plot of Casimir energy per unit area scaled by a^3 vs. the unitless parameter ca^4 between two quadratic potentials $v(z) = cz^2$.

Figure 5.2: Energy Plots for a linear and quadratic potentials.

If one cannot get an exact solution to the differential equation, it is possible to try to calculate the Casimir energy with an approximate solution. In the region of small separation, we would expect that the change in the potential to be small in comparison to the inverse separation. In this region one can try a WKB approximation to the differential equation. An example of this is shown by the dotted line in 5.2(a), notice how the approximation is good for small separation, but breaks down for larger separations.

For the case where the potential is nonzero only for a finite length (mathematically

speaking when the potential has a finite simply connected support) we can use equation (4.45) with $N = 2$, and $A_0(z) = A_2(z) = e^{\kappa z}$ and $B_0(z) = B_2(z) = e^{-\kappa z}$. The reflection coefficient,

$$\widetilde{R} = \frac{1}{\Delta}\Big\{ \big(\kappa B_1(z_1) + B_1'(z_1)\big)e^{\kappa z_1} \int_0^\infty \mathrm{d}z e^{-\kappa z} v(z) A_1(z) \\ - \big(\kappa A_1(z_1) + A_1'(z_1)\big)e^{-\kappa z_1} \int_0^\infty \mathrm{d}z e^{-\kappa z} v(z) B_1(z) \Big\}, \quad (5.10)$$

where Δ is given by

$$\Delta_1^4 = \Big[\big(\kappa A_1(0) - A_1'(0)\big)\big(\kappa B_1(z_1) + B_1'(z_1)\big)e^{\kappa z_1} + \big(\kappa B_1(0) - B_1'(0)\big)\big(\kappa A_1(z_1) + A_1'(z_1)\big)e^{-\kappa z_1} \Big], \quad (5.11)$$

is somewhat unwieldy to work with by hand (which becomes even more true as we add in more and more regions), however it can be easily worked with by a computer algebra system such as *Mathematica* allowing intricate systems to be examined.

For the simplest case where the central potential is a constant potential with a strength σ the reflection coefficient becomes the well known formula,

$$\widetilde{R} = \frac{(\kappa' + \kappa)^2 e^{(\kappa' - \kappa)x_1} - (\kappa' - \kappa)^2 e^{-(\kappa' + \kappa)x_1}}{(\kappa' + \kappa)^2 e^{(\kappa' + \kappa)x_1} + (\kappa' - \kappa)^2 e^{-(\kappa' + \kappa)x_1}}. \quad (5.12)$$

This formula is derived and shown (in a slightly different form) in Milton's 2004 review article [46]. If we let the thickness x_1 of the potential go to zero, $x_1 \to 0$, while increasing the strength of the potential, $\sigma \to \infty$, while holding their product fixed, $\sigma x_1 = \lambda$, we are left with the reflection coefficient

$$\widetilde{R} = \frac{\lambda}{\lambda + 2\kappa}. \quad (5.13)$$

which is the reflection coefficient for a potential represented by a delta function with strength λ, $v(z) = \lambda\delta(z)$.

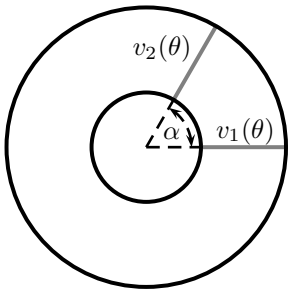

Figure 5.3: An annulus with inner radius a outer radius b, and two semitransparent potentials at $\theta = 0$ and $\theta = \alpha$.

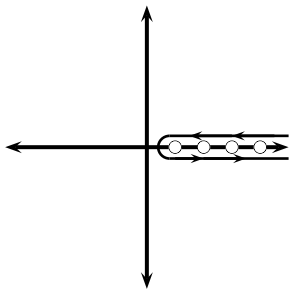

Figure 5.4: The contour γ is defined around the positive real line, while not enclosing zero.

In the limit of very weak coupling $\lambda \to 0$, we can recover relatively simple expressions for the Casimir energy. Two interesting cases are two weakly coupled surfaces,

$$\mathfrak{E} = -\frac{\lambda_1 \lambda_2}{32\pi^2 a}, \tag{5.14}$$

and the interaction between one weakly coupled delta potential and one Dirichlet surface,

$$\mathfrak{E} = -\frac{\lambda}{32\pi^2 a^2}. \tag{5.15}$$

5.2 Non-Planar Geometries: Semi-Transparent Planes in an Annulus

The strength of the results from chapter 3 is that the formulas will work in the set of all separable curvalinear coordinates. As an application we will proceed for a case of two semitransparent planes in the region between two concentric cylinders, as shown in figure 5.3.

This geometry is similar to the wedge geometry first studied in 1978[53, 54], with a

good review by Razmi and Modarresi[55]. However here we include circular boundaries in addition to the wedge boundaries. We will enforce Dirichlet boundary condition on the inner and outer cylinder. This is similar to situations studied globally by Nesterenko *et al* [56, 57] for the case of one circular boundary and locally by Saharian *et al* [58, 59] for the case of both one and two circular boundaries. The potentials will be delta-function potentials in the angular coordinates, $v_1(\theta) = \lambda_1\delta(\theta)$ and $v_2(\theta) = \lambda_2\delta(\theta - \alpha)$. This is most similar to the recent work by Brevik *et al*[60, 61], and Milton *et al*[62].

This problem will be solved using separation of variables as in chapter 3. The energy is then given by equation (3.21). We are taking the ξ_1 coordinates as the azimuthal coordinate θ. This means we will write our reduced Green's function in the azimuthal coordinate, which is different from the traditional way of writing the reduced Green's function in terms of the radial coordinate. The separation constants α_1 and α_2 are the eigenvalues along the axial and radial directions, which we will call k_z and η repectively. From equation (3.21) we can immediately write

$$\mathcal{E} = \frac{1}{4\pi}\int_0^\infty \mathrm{d}\zeta \sum_\eta \ln(1 - \operatorname{tr} g_\eta^{(1)} v_1 g_\eta^{(2)} v_2). \tag{5.16}$$

The Green's function is written in terms of exponential functions and, we find that when enforcing the periodicity requirement,

$$g_\nu^0(\theta,\theta') = \frac{1}{2\nu}\left(-\sinh\nu|\theta-\theta'| + \frac{\cosh\nu\pi}{\sinh\nu\pi}\cosh\nu|\theta-\theta'|\right). \tag{5.17}$$

Using this Green's function in equation (5.16) gives the expression

$$\operatorname{tr} g_\eta^{(1)} v_1 g_\eta^{(2)} v_2 = \frac{\lambda_1\lambda_2\cosh^2\left(\eta(\pi-\alpha)\right)}{(2\eta\sinh\eta\pi + \lambda_1\cosh\eta\pi)(2\eta\sinh\eta\pi + \lambda_2\cosh\eta\pi)}. \tag{5.18}$$

The ηs are the eigenvalues to the modified Bessel equation of purely imaginary order,

$$\left[-r\frac{\partial}{\partial r}r\frac{\partial}{\partial r} + \kappa^2 r^2\right] R_\eta(\kappa r) = \eta^2 R_\eta(\kappa r). \tag{5.19}$$

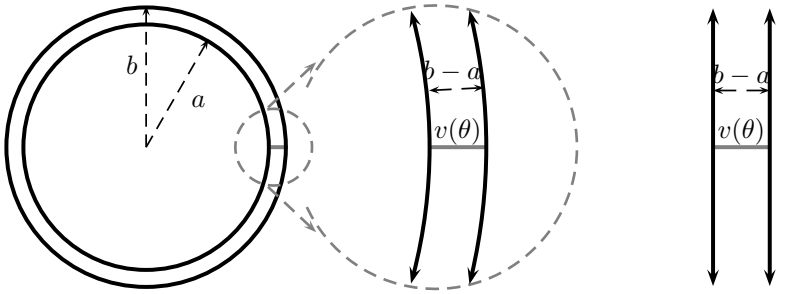

Figure 5.5: If the inner and outer radii are both large in comparison to their separation, we should recover the case of a rectangular piston.

Using the argument principle we can take a complicated sum over eigenvalues and turn it into a path integral around the real line as shown in figure 5.4. For this we need a secular function $D(\eta)$, which is analytic along the real line and has the value zero at the eigenvalues. In this case we define $R_\eta(\kappa a) = 0$, then the eigenvalue condition is given by $D(\eta) = R_\eta(\kappa b)$. The eigenfunction R_η can be written in terms of modified Bessel functions

$$R_\eta(\kappa r) = K_{i\eta}(\kappa a)\widetilde{I}_{i\eta}(\kappa r) - \widetilde{I}_{i\eta}(\kappa a)K_{i\eta}(\kappa r), \tag{5.20}$$

where we define $\widetilde{I}_\eta(x)$ as the part of the modified Bessel function $I_\eta(x)$ even in η.

The energy can be written as

$$\frac{E}{L_z} = \frac{1}{8\pi^2 i}\int_0^\infty \kappa \mathrm{d}\kappa \int_\gamma \mathrm{d}\eta \left[\frac{\partial}{\partial \eta}\ln\left(K_{i\eta}(\kappa a)\widetilde{I}_{i\eta}(\kappa b) - \widetilde{I}_{i\eta}(\kappa a)K_{i\eta}(\kappa b)\right)\right] \times \ln\left(1 - \frac{\lambda_1\lambda_2\cosh^2\left(\eta(\pi-\alpha)\right)}{(2\eta\sinh\eta\pi + \lambda_1\cosh\eta\pi)(2\eta\sinh\eta\pi + \lambda_2\cosh\eta\pi)}\right). \tag{5.21}$$

A quick check of this answer is to look at the limit of large inner and outer radius, as shown in figure 5.5. This should then give the answer for a rectangular piston. For this limit we need the uniform asymptotic expansions of $K_{i\eta}$ and $\widetilde{I}_{i\eta}$, which are worked out by Dunster and Olver [63, 64]. We should also redefine our dimensionless variables in terms of the

dimensionful quantities that will appear in the rectangular piston case, $\widetilde{\eta} = \eta/a$, $\widetilde{\lambda} = \lambda/a$, and $d = \alpha a$. In this asymptotic region we recover the formula for a rectangular piston,

$$\frac{E}{L_z} = \frac{1}{8\pi^2 i}\int_0^\infty \kappa \mathrm{d}\kappa \int_\gamma \mathrm{d}\widetilde{\eta}\left[\frac{\partial}{\partial\widetilde{\eta}}\ln\frac{\sin\left(\sqrt{\widetilde{\eta}^2-\kappa^2}(b-a)\right)}{\sqrt{\widetilde{\eta}^2-\kappa^2}}\right] \times \ln\left(1-\frac{\widetilde{\lambda}_1\widetilde{\lambda}_2 e^{-2\widetilde{\eta}d}}{(2\widetilde{\eta}+\widetilde{\lambda}_1)(2\widetilde{\eta}+\widetilde{\lambda}_2)}\right). \quad (5.22)$$

The path integral simply ensures that $\eta^2 = \kappa^2 + (m\pi/(b-a))^2$.

5.2.1 Numerical Results for Dirichlet Planes

The Casimir energy in equation (5.16) is a quickly converging function so it should be easy to evaluate. However it can be difficult to evaluate the η eigenvalues, which become functions of the wavenumber κ and a natural number m. We can get around this problem by using (5.21). We cannot integrate along the real line because of the poles introduced when we used the argument principle, and we cannot integrate along the imaginary axis because the integral then becomes divergent. So a simple choice is then to let the integration run along the angles of $\pi/4$ and $-\pi/4$. Writing $\mathrm{tr}\, g_\eta^{(1)} v_1 g_\eta^{(2)} v_2 = A(\eta)$ we have

$$\frac{E}{L} = -\frac{1}{4\pi^2}\int_0^\infty \kappa d\kappa \int_0^\infty \mathrm{d}\nu \left\{\frac{\Re R_{\sqrt{i}\nu}\partial_\nu \Re R_{\sqrt{i}\nu} + \Im R_{\sqrt{i}\nu}\partial_\nu \Im R_{\sqrt{i}\nu}}{\left|R_{\sqrt{i}\nu}\right|^2}\arctan\left(\frac{\Im A(\sqrt{i}\nu)}{1+\Re A(\sqrt{i}\nu)}\right) + \frac{\Re R_{\sqrt{i}\nu}\partial_\nu \Im R_{\sqrt{i}\nu} - \Im R_{\sqrt{i}\nu}\partial_\nu \Re R_{\sqrt{i}\nu}}{2\left|R_{\sqrt{i}\nu}\right|^2}\ln\left(1-2\Re A(\sqrt{i}\nu)+\left|A(\sqrt{i}\nu)\right|^2\right)\right\}. \quad (5.23)$$

Here we have used the property that $R_{\eta^*} = R_\eta^*$, and $A(\eta^*) = A^*(\eta)$. The value of $R_{\sqrt{i}\nu}(b,\kappa)$ is obtained as the numerical solution of the differential equation. Using this technique we can obtain a numerical energy in about 1 cpu-second. The results of this calculation are found in figure 5.6(a).

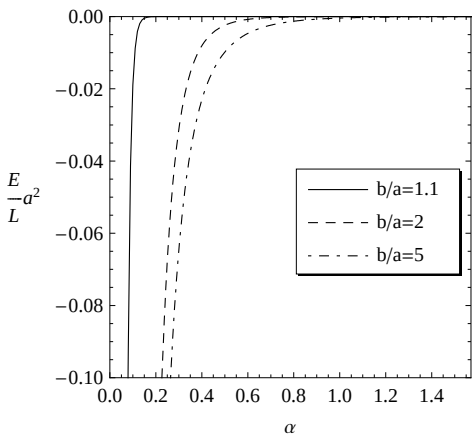

(a) Energy per length vs the angle between the plates. The energy is scaled by the inner radius a.

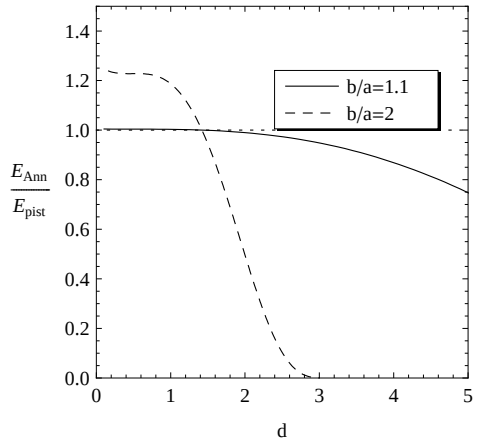

(b) The ratio of the energies of an annular piston to a rectangular piston of similar dimension vs average separation distance between the plates. The separation distance is scaled by the finite size of the piston $b - a$.

Figure 5.6: Casimir energy plots for the annular piston geometry.

Again we would like to compare to known results, so figure 5.6(b) is a graph of the ration of the energies of an annular piston, and a rectangular piston of similar dimension. The rectangular piston is constructed so it has the same finite width $b - a$ as the annular piston, and the separation distance is the mean distance between the annular plates,

$$d = \frac{b-a}{2} 2 \sin\left(\frac{\alpha}{2}\right). \tag{5.24}$$

The results make a certain amount of physical sense. The energy of the annular piston is greater than that of the rectangular piston for small separation because the inner edge of the annular piston is closer, and will contribute more to the energy. However as the annular piston gets further away, the other side of the piston will start to contribute and lower the overall energy. In addition we see that the piston with a small ratio of outer to inner radius is much closer to the rectangular piston for small separations than one with a larger ratio, $E_{\text{ann}}/E_{\text{rect}} \approx 1.004$ for $b/a = 1.1$ vs. $E_{\text{ann}}/E_{\text{rect}} \approx 1.26$ for $b/a = 2$. In both cases the value approached in the plateau in figure 5.6(b) are very close to the ratio of the energies a flat plate vs. a tilted plate predicted by the using proximity force approximation.

Chapter 6

Weak Coupling Expansion: Exact Casimir Energies

The multiple scattering formalism has gained much popularity lately because it has led to a resurgence in Casimir calculations for non-planar geometries. In 2005 Bulgac *et al* calculated the Casimir energy of a Dirichlet sphere in front of a plane [27]. In a series of papers in 2006 Michael Bordag studied the Casimir energy of a cylinder in front of a plane [65] [66] [67]. Most of these papers use the multipole expansion, or something equivalent, which Emig *et al* showed in a series of papers [68] [69] [70] could be generalized to arbitrary shaped separated objects.

6.1 Inspiration: Multipole Expansion

The interaction energy between two bodies translationally invariant in the z direction is given by

$$\mathcal{E} = \frac{1}{4\pi} \int_0^\infty \kappa \mathrm{d}\kappa \, \mathrm{Tr} \ln \left(1 - T_1 \mathcal{G}_0 T_2 \mathcal{G}_\prime\right). \tag{6.1}$$

This is simply a rewriting of the TGTG formula from equation (2.33a).

We will work with two parallel cylindrical shells of radius a and b, their centers a distance R apart as shown in figure 6.1. We will center a separate coordinate system on the axis of each cylinder. The potentials will be given as delta function potentials, $V_1(r) = \lambda_1 \delta(r - a)$

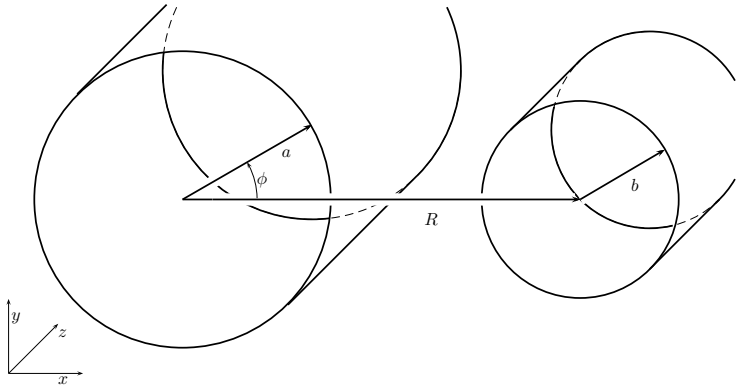

Figure 6.1: Two parallel cylinders of radii a and b, their centers separated by a distance R.

and $V_2(r) = \lambda_2\delta(r-b)$. In these coordinates we can write the free Green's function as

$$\mathcal{G}_0(R + r_\perp - r'_\perp) = \sum_{m,m'=-\infty}^{\infty} \frac{(-1)^m}{2\pi} I_m(\kappa r) e^{im\phi} I_{m'}(\kappa r') e^{im'\phi'} K_{m-m'}(\kappa R). \tag{6.2}$$

The interaction can then be written

$$\mathcal{E} = \frac{1}{4\pi} \int_0^\infty \kappa \mathrm{d}\kappa \ln\det\Big(\delta_{mm'} - \sum_{m''} B_{mm''}(a) B_{m''m'}(b)\Big), \tag{6.3}$$

Where the $B_{mm'}$ matrix is given by

$$B_{mm'}(a) = K_{m+m'}(\kappa R) \frac{\lambda a I^2_{m'}(\kappa a)}{1 + \lambda a I_{m'}(\kappa a) K_{m'}(\kappa a)}. \tag{6.4}$$

The multipole expansion is arrived at by truncating the m sum, and taking the determinant.

Initially we will look at the interaction between Dirichlet cylinders, so we will take the limit at $\lambda_1, \lambda_2 \to \infty$. If we want an analytic expression for small a and b it is easier to expand out the logarithm, yielding the expression

$$\mathcal{E} = -\frac{1}{4\pi R^2} \int_0^\infty x \mathrm{d}x \sum_s \frac{1}{s} \operatorname{Tr} A^s_{m,m'}, \tag{6.5}$$

where the matrix A is

$$A_{mm'} = \sum_{m''=-\infty}^{\infty} K_{m+m''}(x) K_{m''+m'}(x) \frac{I_{m''}(xa/R) I_{m'}(xb/R)}{K_{m''}(xa/R) K_{m'}(xb/R)}. \tag{6.6}$$

The expansion for $I_m(x)/K_m(x)$ starts out at x^{2m} (for $m = 0$ the $K_0(x) \approx \ln(x)$, and $I_0(x) \approx 1$), so for an asymptotic expansion in small a/R, b/R we only have to keep the first few m terms. Keeping only the $m = 0$ term we can derive

$$\mathcal{E} = \frac{1}{8\pi R^2} \frac{1}{\ln(a/R)\ln(b/R)}. \tag{6.7}$$

Working out higher order terms becomes increasingly difficult, as we have to take the determinate of larger and larger matrices.

In the limit of weak coupling ($\lambda_1, \lambda_2 \to 0$), the Casimir energy per unit length is

$$\mathcal{E} = -\frac{\lambda_1 \lambda_2 ab}{4\pi R^2} \sum_{m,m'=-\infty}^{\infty} \int_0^\infty x \mathrm{d}x K_{m+m'}(x) I_{m'}^2(xa/R) I_m^2(xb/R). \tag{6.8}$$

It is relatively simple to work out higher order terms in powers of a/R and b/R, and a pattern is easily recognized,

$$\mathcal{E} = -\frac{\lambda_1 \lambda_2 ab}{8\pi R^2} \sum_{i=0}^{\infty} \left(\frac{a}{R}\right)^{2i} \sum_{j=0}^{i} \binom{i}{j}^2 \left(\frac{b}{a}\right)^{2j}. \tag{6.9}$$

The series of polynomials is easily recognized as A008459 from *Sloane's Online Encyclopedia of Integer Sequences*. The series has a known generating function (see appendix D), so the series can be summed to give an exact closed form energy

$$\mathcal{E} = -\frac{\lambda_1 \lambda_2 ab}{8\pi} \frac{1}{\sqrt{(R+a+b)(R-a-b)(R+a-b)(R-a+b)}}. \tag{6.10}$$

Let us discuss this result for a moment. While this is called an exact result, it is exact only in terms of the geometry; it is still only the lowest order term in an expansion in powers of λ. The closed form nature of the result allows us to very easily study whatever limiting geometry we like, and it provides a good test for the proximity force approximation.

6.2 Weak Coupling Expansion: Point-Wise Summation

The reason the weak coupling expansion gave such a simple expression is that the energy can be expressed as a simple double integral. This can be easily seen by using the TGTG formula, equation (2.36), and expanding in powers of the potential, keeping only the first term. The interaction energy is given by

$$E = -\frac{1}{4\pi}\int \mathrm{d}\zeta \int \mathrm{d}^3x \mathrm{d}^3x' V_1(\vec{x}) G_0(\vec{x},\vec{x}') V_2(\vec{x}') G_0(\vec{x}',\vec{x}) \tag{6.11}$$

The free Helmholtz Green's function for scalar fields is

$$G_0(\vec{x},\vec{x}') = \frac{e^{-\zeta|x-x'|}}{4\pi|x-x'|}. \tag{6.12}$$

So the interaction energy between two potentials is given by

$$E = -\frac{1}{32\pi^3}\int\limits_{V_1} \mathrm{d}^3x \int\limits_{V_2} \mathrm{d}^3x' \frac{V_1(\vec{x})V_2(\vec{x}')}{|x-x'|^3} \tag{6.13}$$

It turns out we can make a similar expansion for the electromagnetic Casimir effect in the limit of dilute dielectrics $(\epsilon - 1) \to 0$. To lowest order in the dielectric constant, the interaction Casimir energy between two dielectric bodies of uniform dielectric constant ϵ_1 and ϵ_2 that occupy distinct volumes V_1 and V_2 respectively is given by

$$E = -\frac{(\epsilon_1-1)(\epsilon_2-1)}{4\pi}\int \mathrm{d}\zeta \int\limits_{V_1} \mathrm{d}^3x \int\limits_{V_2} \mathrm{d}^3x' \,\mathrm{tr}\,\mathbf{\Gamma}_0(\vec{x},\vec{x'}) \cdot \mathbf{\Gamma}_0(\vec{x},\vec{x}'), \tag{6.14}$$

where Γ_0 is the free Green's Dyadic. The free Green's Dyadic for the vector Helmholtz equation is

$$\Gamma_0(\vec{x},\vec{x}') = \zeta^2\big[\mathbf{1} - \nabla\nabla\big]G_0(\vec{x},\vec{x}'). \tag{6.15}$$

Carrying out the ζ integral yields

$$E = -\frac{23(\epsilon_1-1)(\epsilon_2-1)}{(4\pi)^3}\int\limits_{V_1} \mathrm{d}^3x \int\limits_{V_2} \mathrm{d}^3x' \frac{1}{|x-x'|^7}. \tag{6.16}$$

This expression is easily recognizable as the point wise summation of the Casimir-Polder interaction between neutral atoms [5]. This section is a summary of work found in references [71, 72, 73].

The integrals of both cylinders and spheres has worked out in Appendix D.

6.2.1 Cylinders

For two parallel cylindrical shells the as shown in figure 6.1, the Casimir interaction energy per unit length is given by equation (6.10). In the limit of large separation the energy dies off as $1/R^2$,

$$\mathcal{E} = -\frac{\lambda_1 \lambda_2 ab}{8\pi R^2} \quad \text{for } R \gg a, b. \tag{6.17}$$

In the limit of two cylinders almost touching ($d = R - a - b$, and $d \to 0$) we recover the PFA,

$$\mathcal{E} = -\frac{\lambda_1 \lambda_2}{32\pi} \sqrt{\frac{2ab}{(a+b)}} \frac{1}{\sqrt{d}}. \quad \text{for } d \ll b, a. \tag{6.18}$$

From the formula for two cylinders we can take the limit as the radius one of the cylinders goes to infinity. Taking the limit as $R \to \infty$ and $b \to \infty$ but $R - b = L$ fixed we can recover the formula for energy per unit length of a cylindrical shell in front of a weakly coupled wall,

$$\mathcal{E} = \frac{\lambda_1 \lambda_2 a}{16\pi} \frac{1}{\sqrt{(L-a)(L+a)}}. \tag{6.19}$$

If we define $L - a = d$ as the distance from the wall, we can form an expansion in powers of d/a (separation to the radius of curvature of the surface),

$$\mathcal{E} = \frac{\lambda_1 \lambda_2}{32\pi} \sqrt{\frac{2a}{d}} \left(1 - \frac{1}{4}\frac{d}{a} + \frac{3}{32}\frac{d^2}{a^2} - \cdots \right). \tag{6.20}$$

The first term is the PFA, and the further terms are the corrections.

The Casimir interaction energy per unit length for two dilute dielectric cylinders is found by a similar method as with the scalar shells; the integral is expanded in powers of a and b and a generating function is found. The generating function is given in appendix D. The formula for two uniform dilute dielectric cylinders is given by the formula,

$$\mathcal{E} = -\frac{23(\epsilon_1-1)(\epsilon_2-1)a^2b^2}{120\pi}\frac{2R^4 - R^2(a^2+b^2) - (a^2-b^2)^2}{\Big((R+a+b)(R-a-b)(R+a-b)(R-a+b)\Big)^{\frac{5}{2}}}. \tag{6.21}$$

which also reproduces the PFA in the correct limit,

$$\mathcal{E} = -\frac{23(\epsilon_1-1)(\epsilon_2-1)}{5120\pi}\sqrt{\frac{2ab}{a+b}}\frac{1}{d^{\frac{5}{2}}}. \tag{6.22}$$

6.2.2 Spheres

When working with two spherical shells the potentials are given by two delta functions $V_1(r) = \lambda_1\delta(r-a)$ and $V_2(r) = \lambda_2\delta(r-b)$. The Casimir energy for two such spheres with a center to center distance $R > a+b$ is given by the integral

$$E = -\frac{\lambda_1\lambda_2}{16\pi^2}\int_0^{2\pi}\mathrm{d}\phi\int_0^{\pi}\mathrm{d}\theta\int_0^{\pi}\mathrm{d}\theta'\Big(R^2+a^2+b^2-2Ra\cos\theta \\ +2Rb\cos\theta' - 2ab(\cos\theta\cos\theta'+\sin\theta\sin\theta'\cos\phi)\Big)^{-\frac{3}{2}}. \tag{6.23}$$

The general integral of this type is done in appendix D. Fully evaluated, the scalar Casimir energy between two weakly coupled spheres is

$$E = \frac{\lambda_1\lambda_2 ab}{16\pi^2 R}\ln\left(\frac{(R+a+b)(R-a-b)}{(R+a-b)(R-a+b)}\right). \tag{6.24}$$

Two solid dielectric spheres have a corresponding energy

$$E = \frac{23(\epsilon_1-1)(\epsilon_2-1)}{1920\pi^2}\Bigg[\ln\left(\frac{(R+a+b)(R-a-b)}{(R+a-b)(R-a+b)}\right) \\ +4ab\frac{a^6-a^4b^2-a^2b^4+b^6-R^2(3a^4-14a^2b^2+3b^4)+3R^4(a^2+b^2)-R^6}{\Big((R+a+b)(R-a-b)(R+a-b)(R-a+b)\Big)^2} \tag{6.25}$$

6.2.3 Finite Size Planes

(a) Two finite plates, translationally invariant in the z direction in the most general configuration.

(b) One finite plate above an infinite plate, tilted at an angle φ

Figure 6.2: Finite plates tilded with repect to eachother. The plates are translationally invariant in the z direction out of the page.

Two finite ribbons (finite width plates translationally invariant in the z direction) of a general configuration as shown in 6.2(a) yields and expression for the energy in cylindrical coordinates, with origin at the left edge of plate 1,

$$\mathcal{E} = -\frac{\lambda_1\lambda_2}{32\pi^3}\int_0^{L_1} \mathrm{d}r \int_{-d}^{L_2-d} \mathrm{d}x \frac{1}{(x - r\cos\varphi)^2 + (a + r\sin\varphi)^2}. \tag{6.26}$$

This integral can be done exactly, yielding a closed form for the general configuration,

$$\begin{aligned}\mathcal{E} = -\frac{\lambda_1\lambda_2}{32\pi^3\sin\varphi}\Bigg[&\mathrm{Ti}_2\left(\frac{L_2-d}{a}, \cot\varphi\right) - \mathrm{Ti}_2\left(\frac{L_2 - d - L_1\cos\varphi}{a + L_1\sin\varphi}, \cot\varphi\right) \\ &- \mathrm{Ti}_2\left(\frac{-d}{a}, \cot\varphi\right) + \mathrm{Ti}_2\left(\frac{-d - L_1\cos\varphi}{a + L_1\sin\varphi}, \cot\varphi\right)\Bigg],\end{aligned} \tag{6.27}$$

where Ti_2 is the generalized inverse tangent integral,

$$\mathrm{Ti}_2(x, a) = \int_0^x \mathrm{d}y \frac{\arctan y}{y + a}. \tag{6.28}$$

The generalized inverse tangent integral is related to the dialogarithm function, and much information about it can be found the monograph on dialogarithms by Lewin [74].

One simplification would be to let the bottom plate extend off to infinity in both direction ($L_1 \to L$, $L_2 \to \infty$, $d \to -\infty$) as in figure 6.2(b). This is the same geometry as the "Casimir pendulum" problem studied by Scardicchio et al., who used the optical approximation [20].

$$\mathcal{E} = -\frac{\lambda_1 \lambda_2}{32\pi^2 \sin\varphi} \ln\left(\frac{b + \frac{L}{2}\sin\varphi}{b - \frac{L}{2}\sin\varphi}\right). \tag{6.29}$$

This result is exactly that found by the proximity force approximation, if we do not discard the upper limit.

6.2.4 Parallel Plates

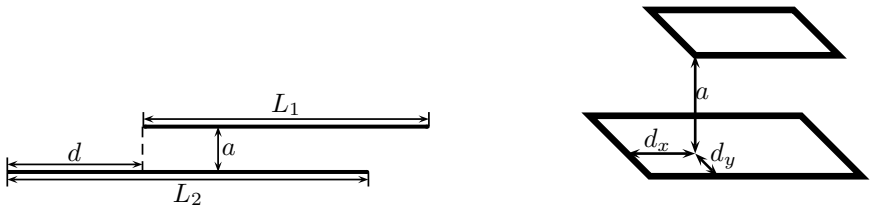

(a) Two finite parallel plates translationally invariant in the z direction out of the page

(b) Two completely finite rectangular plates.

Figure 6.3: Parallel plates

Parallel plates are perhaps the most interesting special case. We can compare the exact expressions for energy and force to those for infinite parallel plates, getting corrections for finite size. In addition, the parallel plates case, due to its simplicity, lends itself well to studying both normal and lateral forces.

Consider the same setup as in the general case shown in 6.2(a), simply letting φ go to zero, as shown in figure 6.3(a). The energy per unit length can be derived directly from (6.27) by using the identity

$$\lim_{a\to\infty} a\,\mathrm{Ti}_2(x,a) = \int \mathrm{d}x \arctan x, \tag{6.30}$$

yielding an integral form for the energy per unit length

$$\mathcal{E} = -\frac{\lambda_1 \lambda_2}{32\pi^3} \left[\int_{\frac{L_2-d-L_1}{a}}^{\frac{L_2-d}{a}} + \int_{\frac{d}{a}}^{\frac{d+L_1}{a}} \right] \mathrm{d}x \arctan x. \tag{6.31}$$

Although an indefinite integral for the arctangent exists, this form is perhaps more illuminating because all the physical quantities are in the limits. The forces, which are given as derivatives of the energy, are all given in terms of arctangents.

Equation (6.31) yields closed forms for the normal force between the plates and the lateral force experienced by the plates by taking the negative derivative with respect to a or d, respectively. The general form of the normal force, defined as $\mathcal{F}_a = -\partial\mathcal{E}/\partial a$, is

$$\mathcal{F}_a = -\frac{\lambda_1 \lambda_2}{32\pi^3 a^2} \left[(L_2 - d) \arctan\left(\frac{L_2 - d}{a}\right) - (L_2 - d - L_1) \arctan\left(\frac{L_2 - d - L_1}{a}\right) \right.$$
$$\left. - d \arctan\left(\frac{d}{a}\right) + (d + L_1) \arctan\left(\frac{d + L_1}{a}\right) \right]. \tag{6.32}$$

In the limiting case of the plates getting very close together we expect to recover the result for the pressure for infinite parallel plates times the area exposed. By mathematically taking $a \to 0$, we use the large argument expansion of the inverse tangent,

$$\arctan(x) = \frac{\pi}{2} - \frac{1}{x} + \frac{1}{3}\frac{1}{x^3} + \cdots, \qquad \text{for } x \to \infty, \tag{6.33}$$

to recover the expected result plus corrections to that result. Because the limiting form of the arctangent depends on the sign of the argument, the single general equation can give several different answers depending on the size and position of the plates. For the situation shown in 6.3(a) the limiting form is

$$\mathcal{F}_a = -\frac{\lambda_1 \lambda_2}{32\pi^2 a^2} \left((L_2 - d) + \mathcal{O}(a^3) \right), \tag{6.34}$$

and the first correction is zero. However, if the plates are the same size and aligned the limiting form of the force with the first correction is

$$\mathcal{F}_a = -\frac{\lambda_1\lambda_2}{32\pi^2 a^2}\left(L - \frac{1}{\pi}2a + \mathcal{O}(a^3)\right). \tag{6.35}$$

If we let one end of both plates extend off into infinity then we can get the edge correction for two aligned plates. This correction is

$$\mathcal{F}_a/\mathcal{F}_0 - 1 = \frac{2a}{\pi L}. \tag{6.36}$$

The general form of the lateral force, similarly defined as $\mathcal{F}_d = -\partial\mathcal{E}/\partial d$, is

$$\mathcal{F}_d = -\frac{\lambda_1\lambda_2}{32\pi^3 a}\Bigg[\arctan\left(\frac{L_2 - d - L_1}{a}\right) - \arctan\left(\frac{L_2 - d}{a}\right) - \arctan\left(\frac{d}{a}\right) + \arctan\left(\frac{d + L_1}{a}\right)\Bigg]. \tag{6.37}$$

From the exact expression for the lateral force, we find there is only one equilibrium position, occurring at $d = \frac{L_1 - L_2}{2}$, where the derivative of the force is negative:

$$\left.\frac{\partial\mathcal{F}_d}{\partial d}\right|_{d=\frac{L_1-L_2}{a}} = -\frac{\lambda_1\lambda_2}{16\pi^3}\frac{L_1 L_2}{\left(a^2 + \left(\frac{L_1+L_2}{2}\right)^2\right)\left(a^2 + \left(\frac{L_1-L_2}{2}\right)^2\right)}, \tag{6.38}$$

signifying a stable equilibrium. The position and qualitative behavior is as expected, the plate have an stable equilibrium when they are symmetrically aligned.

We are also interested in how the lateral force behaves if the plates are very close together. To study that we simply take the limit as $a \to 0$. Assuming without loss of generality that $L_2 > L_1$, to lowest order the force is

$$\mathcal{F}_d = \begin{cases} +\frac{\lambda_1\lambda_2}{16\pi^2 a}, & \text{for } d > 0 \text{ and } d > L_2 - L_1, \\ 0 & \text{for } d > 0 \text{ and } 0 < d < L_2 - L_1, \\ -\frac{\lambda_1\lambda_2}{16\pi^2 a}, & \text{for } d < 0. \end{cases} \tag{6.39}$$

This is what we would expect if we approximated the energy simply as the energy per area between the two infinite plates times the area exposed between the two plates, and took the derivative of this very simple approximation as the force.

6.2.5 Rectangular Parallel Plates

For two rectangular parallel plates, as shown in 6.3(b), the interaction energy is given by the integral

$$E = \frac{-\lambda_1\lambda_2 a}{64\pi^3}\left[\int_{\frac{L_{1x}+d_x-L_{2x}}{a}}^{\frac{L_{1x}+d_x}{a}} + \int_{\frac{d_x}{a}}^{\frac{d_x-L_{2x}}{a}}\right]\mathrm{d}x\left[\int_{\frac{L_{1y}+d_y-L_{2y}}{a}}^{\frac{L_{1y}+d_y}{a}} + \int_{\frac{d_y}{a}}^{\frac{d_y-L_{2y}}{a}}\right]\mathrm{d}y\arctan\left(\frac{xy}{\sqrt{1+x^2+y^y}}\right). \tag{6.40}$$

The two-dimensional indefinite integral in the equation is given by

$$\begin{aligned}\int\mathrm{d}x\int\mathrm{d}y\arctan\left(\frac{xy}{\sqrt{1+x^2+y^2}}\right) &= xy\arctan\left(\frac{xy}{\sqrt{1+x^2+y^2}}\right)\\ &+x\ln\left(x+\sqrt{1+x^2+y^2}\right)+y\ln\left(y+\sqrt{1+x^2+y^2}\right)\\ &-\frac{1}{2}x\ln(1+y^2)-\frac{1}{2}y\ln(1+x^2)-\sqrt{1+x^2+y^2}.\end{aligned} \tag{6.41}$$

The final closed-form expression for the energy of the two rectangular parallel plates is somewhat messy, consisting of the above indefinite integral evaluated at 16 different combinations of variables.

The normal and lateral forces can again be given by the derivatives of the energy with respect to the separation a or to the displacement (this time either d_x or d_y).

The lateral force from the plates has a stable equilibrium when the centers of the two plates are aligned. However, first derivatives of the force can be different for displacements from the equilibrium position in the x and y directions depending on the geometry.

Perhaps the most interesting property of this system as in section 6.2.4 to examine what happens to the attractive force between the plates as the plates get very close together. For very small separations we should get an expression for the force as a power series in a where the first term is the pressure given by the Lifshitz formula times the area between the plates,

$$F_a = -\frac{\lambda_1 \lambda_2}{32\pi^2 a^2} A(1 + c_1 a + c_2 a^2 \cdots). \tag{6.42}$$

Using the large argument expansion for the arctangent (6.33), it is possible to get such an expression for the two plate arrangement, although the expressions for the area and the correction terms depend on the layout of the plates. For a situation in which the upper plate is completely above the lower plate, with none of the edges aligned, the area is given as $A = L_{1x}L_{1y}$ and the first correction term is $c_1 = 0$. For a situation where both plates are the same size, and they are exactly aligned ($d_x = d_y = 0$) then the area is $A = L_x L_y = L_{1x}L_{1y} = L_{2x}L_{2y}$ and

$$c_1 = -\frac{1}{\pi}\frac{2(L_x + L_y)}{L_x L_y} = -\frac{1}{\pi}\frac{\text{Perimeter}}{\text{Area}}. \tag{6.43}$$

The correction term for the case of two parallel disk is exactly the same $c_1 = -\frac{1}{\pi}\frac{\text{Perimeter}}{\text{Area}}$ as was shown by the Wagner *et al*[71]. This suggest that the correction is universal, or independent of shape.

Chapter 7

Conclusions

The two main results from this dissertation come from simplifications to the formula for the Casimir energy for a massless scalar field. These simplified expressions, for separable potentials and weak potentials, are amenable to analytic manipulations as well as dramatically simplified numerical evaluation. This allows us to further the understanding of the Casimir effect in many non-trivial geometries.

We have shown that there is an extreme simplification of the formulas for the Casimir effect of a massless scalar field when we have separable potentials. In the case of planar potentials, or potentials which are a function of a single Cartesian coordinate, we worked out a scalar equivalent to the Lifshitz formula that works for any number of layers and for more potentials given by non-trivial functions of the coordinate. We also worked out a exact expression for the energy of a Casimir piston in an annular region. The expression amenable to analytic manipulation. We could take the limit as the annulus became thin and recover the known result for a rectangular piston. Numerical evaluation of Casimir energy for the annular piston required only 1 cpu-second to calculate to 4 digits of accuracy.

In the case of weak potentials the Casimir energy simplifies to pointwise summation. Because of this simplified expression it is possible to calculate closed form solutions for many geometries. The scalar Casimir energy was calculated between parallel cylindrical shells and spherical shells, and the fully electromagnetic Casimir energy was calculated between solid parallel cylinders and solid spheres made up of a dilute dielectric. We also calculated the

scalar Casimir energy between finite sized ribbons and plates. These closed form solutions allow us to study the range of validity of the proximity force approximation. In the case of parallel ribbons and rectangular parallel plates, we were able to show a consistent correction to the proximity force approximation,

$$F = F_{\mathrm{PFA}}\left(1 - \frac{1}{\pi}\frac{\text{Perimeter}}{\text{Area}} \times \text{Separation} + \cdots\right). \tag{7.1}$$

Bibliography

[1] H. B. G. Casimir. On the Attraction Between Two Perfectly Conducting Plates. *Proc. K. Ned. Akad. Wet.*, 60:793–795, 1948.

[2] R. Eisenschitz and F. London. Über das Verhältnis der van der Waalsschen Kräfte zu den Homöopolaren Bindungskräften. *Z. Phys.*, 60:491–527, 1930.

[3] F. London. Zur Theorie und Systematik der Molekularkräfte. *Z. Phys.*, 63:245–279, 1930.

[4] F. London. Über einige Eigenschaften und Anwendungen der Molekularkräfte. *Z.Phys. Chem.*, B 11:222, 1930.

[5] H. B. G. Casimir and D. Polder. The Influence of Retardation on the London-van der Waals Forces. *Phys. Rev.*, 73:360–372, 1948.

[6] E. M. Lifshitz. The Theory of Molecular Attractive Forces Between Solids. *Sov. Phys. JETP*, 2:73–83, 1956.

[7] I. E. Dzyaloshinskii, E. M. Lifshitz, and L. P. Pitaevskii. The General Theory of van der Waals Forces. *Sov. Phys. Usp.*, 4:153–176, 1961.

[8] J. Schwinger. Casimir Effect in Source Theory. *Lett. Math. Phys.*, 1:43–47, 1975.

[9] Timothy H. Boyer. Quantum Electromagnetic Zero Point Energy of a Conducting Spherical Shell and the Casimir Model for a Charged Particle. *Phys. Rev.*, 174:1764–1774, 1968.

[10] Kimball A. Milton. Semiclassical Electron Models: Casimir Selfstress in Dielectric and Conducting Balls. *Ann. Phys.*, 127:49, 1980.

[11] Jr. DeRaad, Lester L. and Kimball A. Milton. Casimir Selfstress on a Perfectly Conducting Cylindrical Shell. *Ann. Phys.*, 136:229, 1981.

[12] Kimball A. Milton. Fermionic Casimir Stress on a Spherical Bag. *Ann. Phys.*, 150:432, 1983.

[13] Ken Johnson. *unpublished work*, 1983.

[14] Jan Ambjorn and Stephen Wolfram. Properties of the Vacuum. 1. Mechanical and Thermodynamic. *Ann. Phys.*, 147:1, 1983.

[15] Carl M. Bender and Kimball A. Milton. Casimir Effect for a D-Dimensional Sphere. *Phys. Rev.*, D50:6547–6555, 1994.

[16] Kimball A. Milton. Vector Casimir Effect for a D-dimensional Sphere. *Phys. Rev.*, D55:4940–4946, 1997.

[17] B. Derjaguin. Untersuchungen Über die Reibung und Adhäsion, IV. *Kolloid Z.*, 69:155–164, 1934.

[18] Martin Schaden and Larry Spruch. Infinity-free Semiclassical Evaluation of Casimir Effects. *Phys. Rev.*, A58:935–953, 1998.

[19] R. L. Jaffe and A. Scardicchio. The Casimir Effect and Geometric Optics. *Phys. Rev. Lett.*, 92:070402, 2004.

[20] A. Scardicchio and R. L. Jaffe. Casimir Effects: An Optical Approach I. Foundations and Examples. *Nucl. Phys.*, B704:552–582, 2005.

[21] A. Scardicchio and R. L. Jaffe. Casimir Effects: an Optical Approach II. Local Observables and Thermal Corrections. *Nucl. Phys.*, B743:249–275, 2006.

[22] Holger Gies, Kurt Langfeld, and Laurent Moyaerts. Casimir Effect on the Worldline. *JHEP*, 06:018, 2003.

[23] M. J. Renne. Microscopic Theory of Retarded Van der Waals Forces Between Macroscopic Dielectric Bodies. *Physica*, 56:125–137, 1971.

[24] Roger Balian and Bertrand Duplantier. Electromagnetic Waves Near Perfect Conductors. 1. Multiple Scattering Expansions. Distribution of Modes. *Ann. Phys.*, 104:300, 1977.

[25] Roger Balian and Bertrand Duplantier. Electromagnetic Waves Near Perfect Conductors. 2. Casimir Effect. *Ann. Phys.*, 112:165, 1978.

[26] Thorsten Emig. Casimir Forces: An Exact Approach for Periodically Deformed Objects. *Europhys. Lett.*, 62:466–472, 2003.

[27] Aurel Bulgac, Piotr Magierski, and Andreas Wirzba. Scalar Casimir Effect Between Dirichlet Spheres or a Plate and a Sphere. *Phys. Rev.*, D73:025007, 2006.

[28] T. Emig, R. L. Jaffe, M. Kardar, and A. Scardicchio. Casimir Interaction Between a Plate and a Cylinder. *Phys. Rev. Lett.*, 96:080403, 2006.

[29] A. Rodriguez, M. , Ibanescu, D. Iannuzzi, J. D. Joannopoulos, and S. G. Johnson. Virtual Photons in Imaginary Time: Computing Exact Casimir Forces via Standard Numerical Electromagnetism Techniques. *Phys. Rev. A*, 76, 2007.

[30] Sahand Jamal Rahi et al. Nonmonotonic Effects of Parallel Sidewalls on Casimir Forces between Cylinders. *Phys. Rev.*, A77:030101, 2008.

[31] Alejandro W. Rodriguez et al. Stable Suspension and Dispersion-Induced Transitions from Repulsive Casimir Forces Between Fluid-Separated Eccentric Cylinders. *Phys. Rev. Lett.*, 101:190404, 2008.

[32] M. T. Homer Reid, Alejandro W. Rodriguez, Jacob White, and Steven G. Johnson. Efficient Computation of Casimir Interactions between Arbitrary 3D Objects. *Phys. Rev. Lett.*, 103:040401, 2009.

[33] M. J. Sparnaay. Measurements of Attractive Forces Between Flat Plates. *Physica*, 24:751–764, 1958.

[34] E. S. Sabisky and C. H. Anderson. Verification of the Lifshitz Theory of van der Waals Potential Using Liquid Helium Films. *Phys. Rev. A*, 7:791–806, 1973.

[35] P. H. G. M. Blokland and J. T. Overbeek. van der Waals Forces Between Objects Covered with a Chromium Layer. *J. Chem. Soc., Faraday Trans. 1*, 74:2637–2651, 1978.

[36] S. K. Lamoreaux. Demonstration of the Casimir Force in the 0.6 to 6 Micrometers Range. *Phys. Rev. Lett.*, 78:5–8, 1997.

[37] U. Mohideen and Anushree Roy. Precision Measurement of the Casimir Force from 0.1 to 0.9 μm. *Phys. Rev. Lett.*, 81:4549–4552, 1998.

[38] Anushree Roy, Chiung-Yuan Lin, and U. Mohideen. Improved Precision Measurement of the Casimir Force. *Phys. Rev.*, D60:111101, 1999.

[39] R. S. Decca, D. Lopez, E. Fischbach, and D. E. Krause. Measurement of the Casimir Force between Dissimilar Metals. *Phys. Rev. Lett.*, 91:050402, 2003.

[40] R. S. Decca et al. Improved Tests of Extra-Dimensional Physics and Thermal Quantum Field Theory from new Casimir Force Measurements. *Phys. Rev.*, D68:116003, 2003.

[41] R. S. Decca et al. Precise Comparison of Theory and New Experiment for the Casimir Force Leads to Stronger Constraints on Thermal Quantum Effects and Long-Range Interactions. *Annals Phys.*, 318:37–80, 2005.

[42] R. S. Decca et al. Tests of New Physics from Precise Measurements of the Casimir Pressure Between Two Gold-Coated Plates. *Phys. Rev.*, D75:077101, 2007.

[43] R. S. Decca et al. Novel Constraints on Light Elementary Particles and Extra- Dimensional Physics from the Casimir Effect. *Eur. Phys. J.*, C51:963–975, 2007.

[44] Iver H. Brevik, Simen A. Ellingsen, and Kimball A. Milton. Thermal Corrections to the Casimir effect. *New J. Phys.*, 8:236, 2006.

[45] V. B. Bezerra et al. Comment on On the Temperature Dependence of the Casimir Effect. *Phys. Rev.*, E73:028101, 2006.

[46] Kimball A. Milton. The Casimir Effect: Recent Controversies and Progress. *J. Phys.*, A37:R209, 2004.

[47] Michael Bordag, U. Mohideen, and V. M. Mostepanenko. New Developments in the Casimir Effect. *Phys. Rept.*, 353:1–205, 2001.

[48] K. A. Milton. *The Casimir Effect: Physical Manifestations of Zero-Point Energy.* World Scientific, River Edge, USA, 2001.

[49] M. Bordag, G. L. Klimchitskaya, U. Mohideen, and V. M. Mostepanenko. *Advances in the Casimir Effect.* Oxford University Press, New York, 2009.

[50] Oded Kenneth and Israel Klich. Casimir Forces in a T Operator Approach. 2007.

[51] Philip M Morse and Herman Feshbach. *Methods of Theoretical Physics: Part I.* McGraw-Hill, New York, 1953.

[52] P. Moon and Spencer D. E. *Field Thoery Handbook.* Springer-Verlag, Berlin, 1971.

[53] J. S. Dowker and Gerard Kennedy. Finite Temperature and Boundary Effects in Static Space- Times. *J. Phys.*, A11:895, 1978.

[54] D. Deutsch and P. Candelas. Boundary Effects in Quantum Field Theory. *Phys. Rev.*, D20:3063, 1979.

[55] H. Razmi and S. M. Modarresi. Casimir Torque for a Perfectly Conducting Wedge: A Canonical Quantum Field Theoretical Approach. *Int. J. Theor. Phys.*, 44:229–234, 2005.

[56] V. V. Nesterenko, G. Lambiase, and G. Scarpetta. Casimir Effect for a Perfectly Conducting Wedge in terms of Local Zeta Function. *Annals Phys.*, 298:403–420, 2002.

[57] V. V. Nesterenko, I. G. Pirozhenko, and J. Dittrich. Nonsmoothness of the Boundary and the Relevant Heat Kernel Coefficients. *Class. Quant. Grav.*, 20:431–456, 2003.

[58] A. A. Saharian and A. S. Tarloyan. Wightman Function and Scalar Casimir Densities for a Wedge with a Cylindrical Boundary. *J. Phys.*, A38:8763–8780, 2005.

[59] A. A. Saharian and A. S. Tarloyan. Wightman Function and Scalar Casimir Densities for a Wedge with two Cylindrical Boundaries. *Annals Phys.*, 323:1588–1603, 2008.

[60] Iver Brevik, Simen A. Ellingsen, and Kimball A. Milton. Electrodynamic Casimir Effect in a Medium-Filled Wedge. 2009.

[61] Simen Adnoy Ellingsen, Iver Brevik, and Kimball A. Milton. Electrodynamic Casimir Effect in a Medium-Filled Wedge II. 2009.

[62] Kimball A. Milton, Jef Wagner, and Klaus Kirsten. Casimir Effect for a Semitransparent Wedge and an Annular Piston. *Phys. Rev.*, D80:125028, 2009.

[63] T. M. Dunster. Bessel Functions of Purely Imaginary Order, with an Application to Second-Order Linear Differential Equations Having a Large Parameter. *SIAM J. Math. Anal.*, 21:995–1018, 1990.

[64] F. W. J. Olver. *Asymptotics and Special Functions.* Academic Press, New York, 1974.

[65] Michael Bordag. Generalized Lifshitz Formula for a Cylindrical Plasma Sheet in Front of a Plane Beyond Proximity Force Approximation. *Phys. Rev. D*, 75:065003, 2007.

[66] Michael Bordag. The Casimir Effect for a Sphere and a Cylinder in Front of Plane and Corrections to the Proximity Force Theorem. *Phys. Rev. D*, 73:125018, 2006.

[67] Michael Bordag, B Geyer, G. L Klimchitskaya, and V. M. Mostepanenko. Lifshitz-type Formulas for Graphene and Single-Wall Carbon Nanotubes: van der Waals and Casimir Interactions. *Phys. Rev. B*, 74:205431, 2006.

[68] T. Emig, N. Graham, R. L. Jaffe, and M. Kardar. Casimir Forces between Arbitrary Compact Objects. *Phys. Rev. Lett.*, 99:170403, 2007.

[69] T. Emig, N. Graham, R. L. Jaffe, and M. Kardar. Casimir Forces between Compact Objects: I. The Scalar Case. *Phys. Rev.*, D77:025005, 2008.

[70] T. Emig and R. L. Jaffe. Casimir Forces Between Arbitrary Compact Objects: Scalar and Electromagnetic Field. *J. Phys.*, A41:164001, 2008.

[71] Jef Wagner, Kimball A. Milton, and Prachi Parashar. Weak Coupling Casimir Energies for Finite Plate Configurations. *J. Phys. Conf. Ser.*, 161:012022, 2009.

[72] Kimball A. Milton, Prachi Parashar, and Jef Wagner. Exact Results for Casimir Interactions between Dielectric Bodies: The Weak-Coupling or van der Waals Limit. *Phys. Rev. Lett.*, 101:160402, 2008.

[73] Kimball A. Milton and Jef Wagner. Exact Casimir Interaction Between Semitransparent Spheres and Cylinders. *Phys. Rev.*, D77:045005, 2008.

[74] Leonard Lewin. *Polylogarithms and Associated Functions.* New York, Oxford: North Holland, 1981.

[75] Kimball A. Milton, Prachi Parashar, Jef Wagner, and K. V. Shajesh. Exact Casimir Energies at Nonzero Temperature: Validity of Proximity Force Approximation and Interaction of Semitransparent Spheres. 2009.

[76] G. G. J. Jacobi. Untersuchungen über die Differentialgleichung der Hypergeometrishen Reihe. *J. Reine Ange. Math.*, 56:149–165, 1859.

[77] P. L. Tchebychef. Sur les Fonctions Analogues à Celles de Legendre. *Zap. Akad. Nauk*, 16:131–140, 1870.

[78] Richard Askey. Jacobi's Generating Function for Jacobi Polynomials. *Proc. Am. Math. Soc.*, 71:243–246, 1978.

Appendix A

Properties and Identities for Sturm-Liouville Operators

A.1 Properites of Sturm-Liouville Systems

This section is just reminder of the properties of a Sturm-Liouville system. Many of these properties are used throughout the dissertation, especially in chapter 4. A Sturm-Liouville differential equaiton has the form

$$\Big(-\frac{\partial}{\partial x} p(x) \frac{\partial}{\partial x} + q(x) \Big) y(x) = \lambda^2 r(x) y(x), \tag{A.1}$$

where x is in some interval $[a, b]$. We have the additional conditions that $p(x), r(x) > 0$, and $p(x), p'(x), q(x)$, and $r(x)$ are continuous in the region (a, b).

As a consequence of the Sturm-Liouville theorem the solutions exist and the eigenvalues of the system are real, distinct, and bounded below,

$$\lambda_0 < \lambda_1 < \cdots < \lambda_n < \cdots . \tag{A.2}$$

For each eigenvalue there is a distinct eigenfunction $u_{\lambda_i(x)}$, and these eigenfunctions can be made to be orthonormal,

$$\int r(x) \mathrm{d}x u_{\lambda_i}(x) u_{\lambda_j}(x) = \delta_{i,j}. \tag{A.3}$$

In addition to the standard results from Sturm-Liouville theory, many other useful properties can be shown.

A.1.1 Wronksian Proof

In chapter 4 it is stated that the Wronskian times the weight $p(x)$ is a constant. If the Wronskian times the weight function is a constant then its derivative with respect to x must be zero.

Proof. Let $u(x)$ and $v(x)$ be two independent solutions that satisfy (A.1).

$$\begin{aligned}
\frac{\mathrm{d}}{\mathrm{d}x}\left(p(x)W[u,v](x)\right) &= \frac{\mathrm{d}}{\mathrm{d}x}\left(p(x)u(x)\frac{\mathrm{d}}{\mathrm{d}x}v(x) - p(x)v(x)\frac{\mathrm{d}}{\mathrm{d}x}u(x)\right) \\
&= u(x)\frac{\mathrm{d}}{\mathrm{d}x}p(x)\frac{\mathrm{d}}{\mathrm{d}x}v(x) - v(x)\frac{\mathrm{d}}{\mathrm{d}x}p(x)\frac{\mathrm{d}}{\mathrm{d}x}u(x) \\
&= u(x)\big(q(x) - \lambda^2 r(x)\big)v(x) - v\big(q(x) - \lambda^2 r(x)\big)u(x) \\
&= 0.
\end{aligned}$$

Q.E.D

A.1.2 Integral Theorem

It is often neccesary to integrate a product of solutions to a Sturm-Liouville differential equation, such as needed in section 3.2. For any two solutions u and v (they can even be the same solution)

$$ruv = -\frac{1}{2\lambda}\frac{\partial}{\partial x}\left[p\left(u\frac{\partial}{\partial x}\frac{\partial}{\partial \lambda}v - \frac{\partial}{\partial x}u\frac{\partial}{\partial \lambda}v\right)\right]. \tag{A.4}$$

Proof.

$$\begin{aligned}
&\frac{\partial}{\partial x}\left[p\left(u\frac{\partial}{\partial x}\frac{\partial}{\partial \lambda}v - \frac{\partial}{\partial x}u\frac{\partial}{\partial \lambda}v\right)\right] \\
&= u\frac{\partial}{\partial \lambda}\left[\frac{\partial}{\partial x}\left(p\frac{\partial}{\partial x}v\right)\right] - \left[\frac{\partial}{\partial x}\left(p\frac{\partial}{\partial x}u\right)\right]\frac{\partial}{\partial \lambda}v \\
&= u\frac{\partial}{\partial \lambda}(q-\lambda^2 r)v - (q-\lambda^2 r)u\frac{\partial}{\partial \lambda}v \\
&= -2\lambda ruv.
\end{aligned}$$

Q.E.D

Appendix B

Solving a Tri-Diagonal Matrix Equation

In this section we will solve a general tri-diagonal matrix equation of the form

$$\begin{pmatrix} b_1 & c_1 & & & \\ a_2 & b_2 & c_2 & & \\ & \ddots & \ddots & \ddots & \\ & & a_n & b_n \end{pmatrix} \begin{pmatrix} x_1 \\ x_2 \\ \vdots \\ x_n \end{pmatrix} = \begin{pmatrix} d_1 \\ d_2 \\ \vdots \\ d_n \end{pmatrix}. \tag{B.1}$$

We will define a short-hand notation for a tri-diagonal matrix

$$M_i^j = \begin{pmatrix} b_i & c_j & & \\ a_{i+1} & \ddots & \ddots & \\ & \ddots & \ddots & c_{j-1} \\ & & a_j & b_j \end{pmatrix} \tag{B.2}$$

where the i and j signify the appropriate beginning and ending terms of the sequences $\{a\}$, $\{b\}$, and $\{c\}$. We will also define the notation

$$M_1^n(i) = \begin{pmatrix} b_1 & c_1 & & d_1 & & \\ a_2 & \ddots & c_{i-2} & & & \\ & \ddots & b_{i-1} & & & \\ & & a_i & & c_i & \\ & & & & b_{i+1} & \ddots \\ & & & & a_{i+2} & \ddots & c_{n-1} \\ & & & d_n & & a_n & b_n \end{pmatrix} \tag{B.3}$$

for a matrix with the i^{th} column replaced by the target vector $\vec{d}$. Using this shorthand notation we can easily write the i^{th} entry in the solution vector $\vec{x}$ using Kramer's rule,

$$x_i = \frac{\det\left(M_1^n(i)\right)}{\det\left(M_1^n\right)}. \tag{B.4}$$

We can write the determinant of the matrix $M_1^n(i)$ as a sum of determinants of the minors, expanding down the replaced column. Because we expand the determinant down the

replaced column, the minors of $M_1^n(i)$ are the same as the minors of the original matrix M_1^n,

$$\det\left(M_1^n(i)\right) = (-1)^i \sum_{j=1}^{n} (-1)^j \det\left(\text{minor}\left(M_1^n\right)_{j,i}\right) d_j. \tag{B.5}$$

The j, i^{th} minor is the matrix M_1^n with the i^{th} column and j^{th} row removed.

When $j < i$ the matrix would still have three diagonals with nonzero components, with the diagonals below the now missing row j and left of column i shifted up by one. In this particular case we can represent the matrix by,

$$\text{minor}\left(M_1^n\right) = \left(\begin{array}{cccccc} & & c & & & \\ & b & & c & & \\ a & & b & & c & \\ & a & & b & & c \\ & & & & b & \\ & & & & a & \end{array} \right). \tag{B.6}$$

The missing row j and column i are represented by the solid horizontal and vertical lines in equation (B.6). We will also divide the matrix between the $(j-1)^{\text{th}}$ and j^{th} column, and the i^{th} and $(i-1)^{\text{th}}$ row, as shown by dotted lines in equation (B.6). This division gives us a block form for the matrix that is square along the diagonal and upper triangular. We can write the minor of the tri-diagonal matrix in block matrix form

$$\text{minor}\left(M_1^n\right)_{i,j} = \begin{pmatrix} M_1^{j-1} & \overline{c}_{j-1} & 0 \\ 0 & \mathcal{A}_{j+1,i} & \overline{c}_i \\ 0 & 0 & M_{i+1}^n \end{pmatrix} \quad \text{where} \quad \mathcal{A}_{i,j} = \begin{pmatrix} a_i & b_i & c_i & & \\ & & & c_{j-2} & \\ & & & & b_{j-1} \\ & & & & a_j \end{pmatrix}, \tag{B.7}$$

and the $\overline{c}_i$s are matrices with just 1 entry c_i in the lower left corner.

A similar construction will give us the form of the minor for $j > i$,

$$\text{minor}\,(M_1^n)_{i,j} = \begin{pmatrix} M_1^{i-1} & 0 & 0 \\ \overline{a}_i & \mathcal{C}_{i,j-1} & 0 \\ 0 & \overline{a}_{j+1} & M_{j+1}^n \end{pmatrix} \quad \text{where} \quad \mathcal{C}_{i,j} = \begin{pmatrix} c_i & & \\ b_{i+1} & \ddots & \\ a_{i+2} & \ddots & \ddots \\ & a_j & b_j & c_j \end{pmatrix}, \quad \text{(B.8)}$$

and $\overline{a}_i$ are matrices with just 1 entry a_i in the upper right corner. For $i = j$ the minor is simply block diagonal

$$\text{minor}\,(M_1^n)_{i,i} = \begin{pmatrix} M_1^{i-1} & 0 \\ 0 & M_{i+1}^n \end{pmatrix}. \quad \text{(B.9)}$$

We can now use a major simplification: the determinant of block triangular matrices can be written as a product of the determinants of the blocks along the diagonal. In the case of matrices which are triangular (not just block triangular), such as $\mathcal{A}$ or $\mathcal{C}$, the determinant is just the product of the diagonal coefficients. We can now write the solution x_i in a sufficiently compact and easy to calculate form,

$$x_i = \frac{1}{\det(M_1^n)} \left((-1)^i \sum_{j=1}^{i-1} (-1)^j d_j \det(M_1^{j-1}) \det(M_{i+1}^n) \prod_{m=j+1}^{i} a_m \right.$$
$$\left. + d_i \det(M_1^{i-1}) \det(M_{i+1}^n) + (-1)^i \sum_{j=i+1}^{n} (-1)^j d_j \det(M_1^{i-1}) \det(M_{j+1}^n) \prod_{m=i}^{j-1} c_m \right). \quad \text{(B.10)}$$

B.1 Delta Recursion Relation Proof

In section 4.1.3, it is stated without proof the determinants of the tridiagonal matrix can be simplified with a redefinition in terms of Δ terms that obey a simple resursion formula. The result is attained rather quickly using induction.

Proof. For $i = 1, 2, 3$ we have

$$\begin{aligned}
\det(M_1^1) &= \Delta_1^1 = b_1 \quad \therefore \\
\det(M_1^2) &= b_2 b_1 - a_2 c_1 \\
&= (-a_1)\left(\Delta_1^2 = \widetilde{c}_2\right) \quad \therefore \\
\det(M_1^3) &= b_3(-a_1\widetilde{c}_2) - a_3 c_2 b_1 \\
&= (-a_1)\left(\Delta_1^3 = b_3\widetilde{c}_2 + a_3 b_1\right) \quad \therefore . \qquad \text{(B.11)}
\end{aligned}$$

The inductive step assuming equation (4.36),

$$\begin{aligned}
\det(M_1^{2i+2}) &= -\widetilde{c}_{2i+2} a_{2i+1} \det(M_1^{2i}) - b_{2i+2} a_{2i+1} c_{2i} \det(M_1^{2i-1}) \\
&= (-a_{2i+1}) \textstyle\prod_{j=1}^{i} (-a_{2j-1}) \widetilde{c}_{2i+2} \Delta_1^{2i} - (-a_{2i+1})(-a_{2i-1}) \prod_{j=1}^{i-1} (-a_{2j-1}) b_{2i+2} \Delta_1^{2i-1} \\
&= \prod_{j=1}^{i+1} (-a_{2j-1}) \left(\Delta_1^{2i+2} = \widetilde{c}_{2i+2}\Delta_1^{2i} - b_{2i+2}\Delta_1^{2i-1}\right) \quad \therefore \\
\det(M_1^{2i+3}) &= b_{2i+3} \det(M_1^{2i+2}) - a_{2i+3} c_{2i+2} \det(M_1^{2i+1}) \\
&= \textstyle\prod_{j=1}^{i+1} (-a_{2j-1}) b_{2i+3} \Delta_1^{2i+2} - (-a_{2i+1}) \prod_{j=1}^{i} (-a_{2j-1}) a_{2i+3} \Delta_1^{2i+1} \\
&= \prod_{j=1}^{i+1} (-a_{2j-1}) \left(\Delta_1^{2i+3} = b_{2i+3}\Delta_1^{2i+2} + a_{2i+3}\Delta_1^{2i+1}\right) \quad \therefore . \qquad \text{(B.12)}
\end{aligned}$$

The $\therefore$ symbols show the initial terms, and the recursion relation for the Δs. **Q.E.D**

Appendix C

Proximity Force Approximation

Casimir calculations with non-parallel planar geometries are very difficult, often impossible, to do exactly. The proximity force approximation (FPA) is most often used for these cases. The PFA is used when we have a formula for the force per area (or energy per area) between two parallel planar surfaces, and we would like it between two non-parallel surfaces. The PFA states that the total energy is given by the sum of the energies of infinitesimal parallel surfaces,

$$E = \int \mathrm{d}A \mathfrak{E}(h). \tag{C.1}$$

The proximity force theorem states that if $\mathfrak{E}(h)$ dies off fast enough then the exact energy approaches the PFA as the distance between the surfaces approaches zero. However it should be noted that there is no standard way of getting an error term for the PFA, which limits its value.

We will examine three cases explicitly in this appendix: Tilted planes with the geometry shown in figure C.1(a), and parallel cylinders and spheres, with the geometry shown in figure C.1(b). In all cases we will define d as the distance of closest approach, giving

$$h = d + x \sin \varphi, \tag{C.2}$$

for the tilted planes, and

$$h = d + a(1 - \cos\theta) + b(1 - \cos\theta'), \tag{C.3}$$

for both the parallel cylinders and spheres. In the case of the curved surfaces we need to θ'

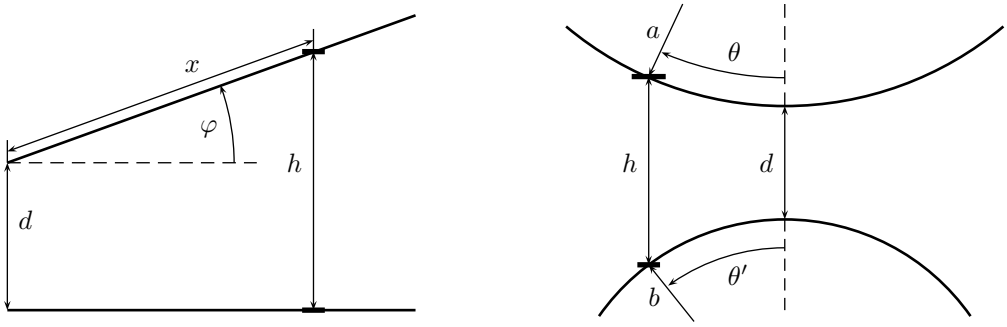

(a) Two planar surfaces tilted at an angle φ.

(b) Two curved surfaces. θ

Figure C.1: Figures explaning the coordinates and variable used in the proximity force approximation calculations.

in terms of θ, which can be easily seen from figure C.1(b) to be

$$a \sin\theta = b \sin\theta'. \tag{C.4}$$

Also for the case of simplicity we will assume that the energy per unit area $\mathfrak{E}$ is given by a simple power law,

$$\mathfrak{E}(h) = \frac{k}{h^p}, \tag{C.5}$$

which is the case for Dirichlet surfaces, or weakly coupled delta function planes.

C.1 Tilted Surfaces

For the case of tilted surfaces we can only integrate out one perpendicular direction, leaving us with a energy per unit length $\mathcal{E}$. The PFA gives

$$\mathcal{E} = \int_0^L \mathrm{d}x \mathfrak{E}(h). \tag{C.6}$$

For an energy per unit area given by a power law as in equation (C.5) the PFA integrates out to give

$$\mathcal{E} = \frac{k}{\sin\varphi}\frac{1}{d^{p-1}(p-1)}, \tag{C.7}$$

where we have thrown away the upper limit, since it is finite as $d \to 0$ for $\varphi \neq 0$.

C.2 Curved Surfaces

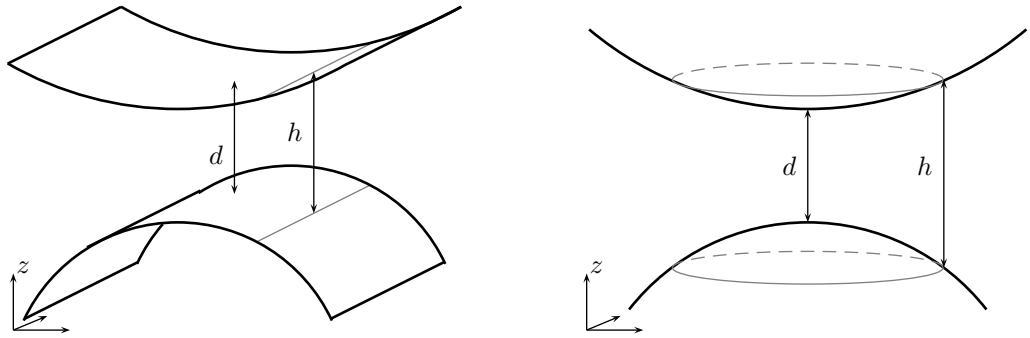

(a) Two parallel cylinders.

(b) Two spheres.

Figure C.2: more detailed figures showing the coordinates for curved surfaces.

For parallel cylinders as shown in figure C.2(a) the PFA gives

$$\mathcal{E} = a\int_{-\pi/2}^{\pi/2} \mathrm{d}\theta\, \mathfrak{E}(h). \tag{C.8}$$

To evaluate the integral for a power law, we have to make a small angle approximation, which redefines h to be

$$h = d + \frac{1}{2}\left(\frac{ab(a+b)}{b^2}\right)\theta^2. \tag{C.9}$$

The PFA then gives a energy per unit length of

$$\mathcal{E} = k\sqrt{\frac{2ab}{a+b}}\frac{1}{d^{p-\frac{1}{2}}}B\left(\tfrac{1}{2}, p-\tfrac{1}{2}\right), \tag{C.10}$$

where $B(x, y)$ is the Euler beta function. For the case of a single curved surface in front of a flat surface, we can simply take the limit as one of radii gets very large ($b \to \infty$), giving

$$\mathcal{E} = k\frac{\sqrt{2a}}{d^{p-\frac{1}{2}}}B\left(\tfrac{1}{2}, p-\tfrac{1}{2}\right), \tag{C.11}$$

For two spheres as shown in figure C.2(b) the PFA gives an energy of

$$E = 2\pi a^2 \int_0^{\pi/2} \sin\theta \mathrm{d}\theta \mathfrak{E}(h). \tag{C.12}$$

Using a power law the energy is given by

$$E = k\frac{2\pi ab}{(p-1)(a+b)}\frac{1}{d^{p-1}}. \tag{C.13}$$

Also for the case of a single sphere in front of a plane we can write

$$E = k\frac{2\pi a}{(p-1)d^{p-1}}. \tag{C.14}$$

Appendix D

Mean Powers of Distance

Using the multiple scattering formalism, we have shown that the weak coupling calculations are equivalent to the pairwise summation. So all calculations, either for scalar fields or E&M fields take on the form

$$E = k \int_{V_1} \int_{V_2} \frac{\mathrm{d}^3 r_1 \mathrm{d}^3 r_2}{|\vec{r}_1 - \vec{r}_2|^p}, \tag{D.1}$$

for constant k and some power p. The integral alone is the mean powers of distance between two bodies V_1 and V_2. This work was motivated when looking into the tempurature dependence of the Casimir effect in curved geometries in a recent paper [75].

In this section we will work out the mean powers of the distance between two spheres or two parallel cylinders. However it should be noted that this is not a formal proof, we have not shown that the expansions of the interal equal the series we suppose. By inspection of the initial terms in the series we simply guessed a formula. A nontrivial check is that the integrated forms give the correct PFA in the limit of objects touching $(a + b) \to R$.

D.1 Two Spherical Shells

We can start off with two spherical shells, in the arrangement shown in figure D.1. From the figure, it is easy to write down the coordinates on the surface,

$$x = a\sin\theta\cos\phi \qquad y = a\sin\theta\sin\phi \qquad z = a\cos\theta$$

$$x' = b\sin\theta'\cos\phi' \qquad y' = b\sin\theta'\sin\phi' \qquad z' = R + b\cos\theta,$$

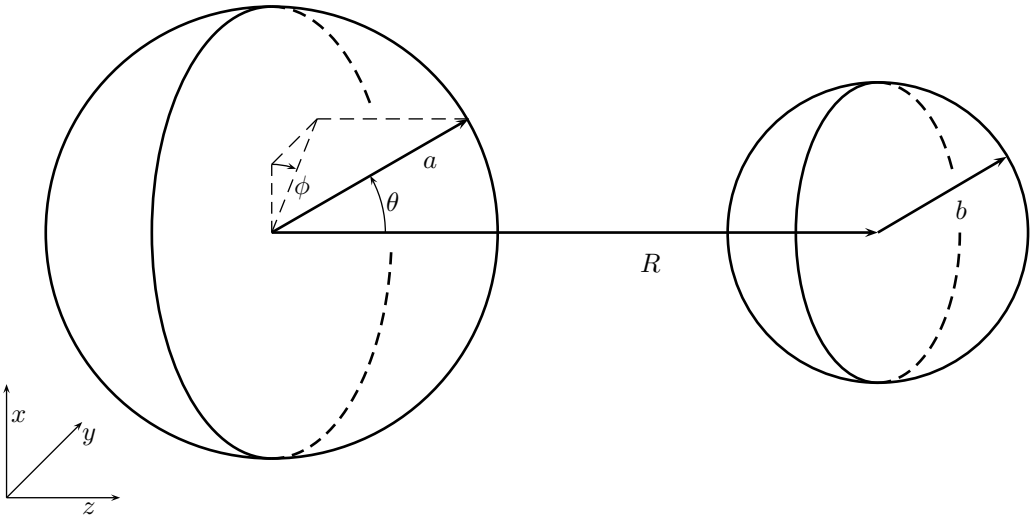

Figure D.1: Two spherical shells of radii a and b, with their centers separated by a distance R.

which gives a mean distance $\hat{D}$ defined as

$$\hat{D}_p(R,a,b) = \int_0^\pi \sin\theta \mathrm{d}\theta \int_0^\pi \sin\theta' \mathrm{d}\theta' \int_0^{2\pi} \mathrm{d}\phi \int_0^{2\pi} \mathrm{d}\phi' \Big\{ R^2 + a^2 + b^2 - 2Ra\cos\theta + 2Rb\cos\theta' - 2ab\big[\cos\theta\cos\theta' + \sin\theta\sin\theta'\cos(\phi-\phi')\big]\Big\}^{-\frac{p}{2}}. \quad \text{(D.2)}$$

We can immediately pull out an overall R^{-p}, and scale both a and b by R. We will define this scaled quantity as $D_p(\hat{a},\hat{b}) = R^p \hat{D}_p(R,a,b)$, where $\hat{a} = a/R$ and $\hat{b} = b/R$. From here on we will drop the hats on a and b for readablilty. We will expand the integrand in powers of a and b,

$$\Big\{1 + a^2 + b^2 - 2a\cos\theta + 2b\cos\theta' - 2ab\big[\cos\theta\cos\theta' + \sin\theta\sin\theta'\cos(\phi-\phi')\big]\Big\}^{-\frac{p}{2}} = \sum_{i,j=0}^{\infty} A_{i,j} a^i b^j. \quad \text{(D.3)}$$

This expansion is bounded above by a binomial expansion with $(a+b)$ as the variable, and because $a+b<1$ (the spheres do not touch or overlap) this sum converges. We can exchange the order of the sum and the integral because of the convergence properties, and define the term $B_{i,j}$ as

$$B_{i,j} = \int_0^\pi \sin\theta \mathrm{d}\theta \int_0^\pi \sin\theta' \mathrm{d}\theta' \int_0^{2\pi} \mathrm{d}\phi \int_0^{2\pi} \mathrm{d}\phi' A_{i,j}. \tag{D.4}$$

Using a computer algebra system (*Mathematica*) to do the first several terms by hand we come the conclusion that $B_{i,j}=0$ for all i or j odd. From the first several non-zero terms we can identify a pattern and write a formula for i and j even,

$$B_{i,j} = 16\pi^2 \frac{1}{(i+1)!(j+1)!} \prod_{k=1}^{i+j} (p+k-2). \tag{D.5}$$

By reordering the summation, and excluding the zero terms we can write

$$D_p(a,b) = \frac{16\pi^2}{\Gamma(p-1)} \sum_{i=0}^{\infty} \sum_{j=0}^{i} \frac{\Gamma(p+2i-1)}{(2i-2j+1)!(2j+1)!} a^{2i-2j} b^{2j}. \tag{D.6}$$

This expression can be completely resummed yielding,

$$D_p(a,b) = \frac{1}{4ab(p-2)(p-3)} \Big[(1+a+b)^{3-p} + (1-a-b)^{3-p} - (1+a-b)^{3-p} - (1-a+b)^{3-p} \Big]. \tag{D.7}$$

Now this equation is valid for any $p \neq 2,3$, so we can just take a limit as $p \to 2$ or $p \to 3$ in those instances.

D.1.1 Solid Spheres

For the interaction of a spherical shell of radius a and a solid sphere of radius b we would write,

$$D_p^{S\delta}(a,b) = \int_0^b r^2 \mathrm{d}r D_p(a,r). \tag{D.8}$$

The following formulas are quite long, and it is useful to adapt a shorthand notation ($\pm\pm$) to mean $(1 \pm a \pm b)$. Using this shorthand we can write

$$D_p^{S\delta}(a,b) = \frac{4\pi^2}{\prod_{k=2}^{4}(k-p)}\Bigg\{\frac{b}{a}\Big[(++)^{4-p} - (--)^{4-p} - (+-)^{4-p} + (-+)^{4-p}\Big] - \frac{1}{a(5-p)}\Big[(++)^{5-p} + (--)^{5-p} - (+-)^{5-p} - (-+)^{5-p}\Big]\Bigg\}. \quad \text{(D.9)}$$

Similarly if we integrate out both variables we can get an expression for the mean powers of distance between two solid spheres,

$$D_p^{SS}(a,b) = \frac{4\pi^2}{\prod_{k=2}^{5}(k-p)}\Bigg\{ab\Big[(++)^{5-p} + (--)^{5-p} + (+-)^{5-p} + (-+)^{5-p}\Big] - \frac{a+b}{6-p}\Big[(++)^{6-p} - (--)^{6-p}\Big] + \frac{a-b}{6-p}\Big[(+-)^{6-p} - (-+)^{6-p}\Big] + \frac{1}{(7-p)(6-p)}\Big[(++)^{7-p} + (--)^{7-p} - (+-)^{7-p} - (-+)^{7-p}\Big]\Bigg\}. \quad \text{(D.10)}$$

D.2 Two Cylindrical Shells

When we work with two parallel cylindrical shells as shown in figure D.2, we can write the formula for mean powers of distance as

$$\hat{D}_p(R,a,b) = \int_0^{2\pi}\mathrm{d}\phi\int_0^{2\pi}\mathrm{d}\phi'\int_{-\infty}^{\infty}\mathrm{d}z\int_{-\infty}^{\infty}\mathrm{d}z'\Big\{R^2 + a^2 + b^2 - 2Ra\cos\phi + 2Rb\cos\phi' - 2ab\cos(\phi-\phi') + (z-z')^2\Big\}^{-\frac{p}{2}}. \quad \text{(D.11)}$$

First we integrate out the z component to get a mean distance per unit length $\int \mathrm{d}z\mathcal{D}_p(\hat{a},\hat{b}) = R^{p+1}\hat{D}_p(R,a,b)$, where again $\hat{a} = a/R$ and $\hat{b} = b/R$. Like the case for sphere we will drop the hat notation for a and b for readability. Unlike the case for spheres which is valid for

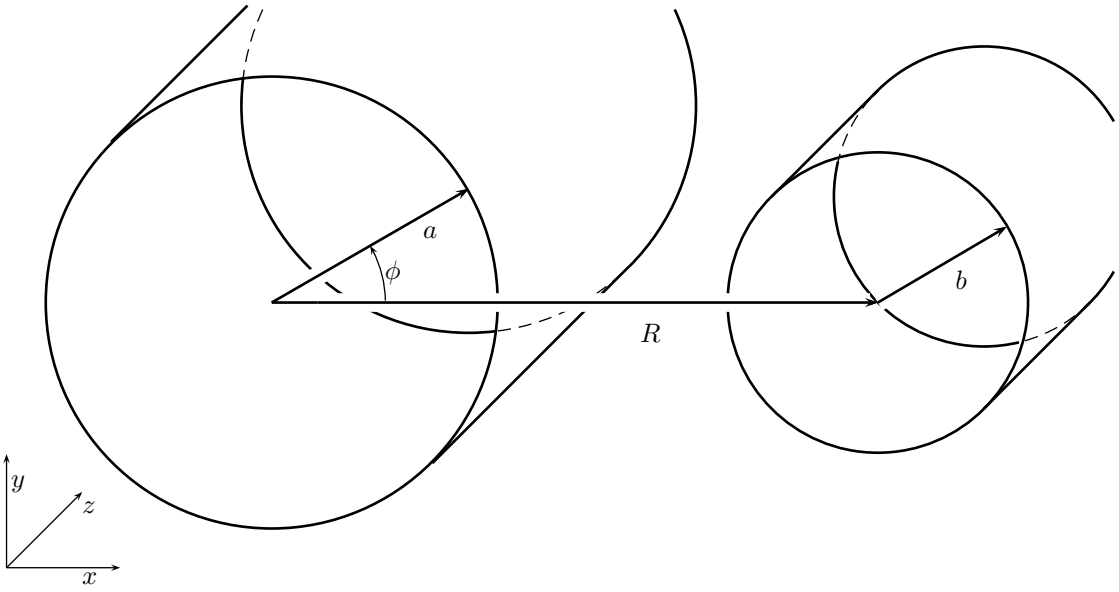

Figure D.2: Two cylindrical shells of radii a and b, with their centers separated by a distance R.

all powers p, this integral only converges for $p > 1$ yielding

$$\mathcal{D}_p(a,b) = \frac{\sqrt{\pi}\Gamma\left(\frac{p-1}{2}\right)}{\Gamma\left(\frac{p}{2}\right)} \int_0^{2\pi} \mathrm{d}\phi \int_0^{2\pi} \mathrm{d}\phi' \Big\{ 1 + a^2 + b^2 - 2a\cos\phi + 2b\cos\phi' - 2ab\cos(\phi - \phi') \Big\}^{\frac{1-p}{2}}. \quad \text{(D.12)}$$

Similar to the sphere case we can now expand the integrand in powers of a and b, and integrate out the angular coordinates. Also similar to the case with two spheres we are only left with even powers of a and b (all terms with odd powers integrated to zero). From the first several rows of nonzero terms we can identify the pattern

$$\mathcal{D}_p(a,b) = \frac{4\pi^{5/2}}{\Gamma\left(\frac{p}{2}\right)\Gamma\left(\frac{p-1}{2}\right)} \sum_{i=0}^{\infty} \sum_{j=o}^{i} \frac{\Gamma\left(\frac{p-1}{2} + i\right)^2}{\big((i-j)!\big)^2 (j!)^2} a^{2i-2j} b^{2j}. \quad \text{(D.13)}$$

The rows can be recognized as Sloane's A008459, which gives the formula for the rows as

$$\sum_{j=0}^{i} \binom{i}{j}^2 x^j = (1-x)^i P_i\left(\frac{1+x}{1-x}\right), \tag{D.14}$$

where $P_i(x)$ is the i^{th} order Legendre polynomial. This gives use the expression

$$\mathcal{D}_p(a,b) = \frac{4\pi^{5/2}}{\Gamma\left(\frac{p}{2}\right)\Gamma\left(\frac{p-1}{2}\right)} \sum_{i=0}^{\infty} \frac{\Gamma\left(\frac{p-1}{2}+i\right)^2}{(i!)^2} (a^2-b^2)^i P_i\left(\frac{a^2+b^2}{a^2-b^2}\right). \tag{D.15}$$

This final expression can be summed to a closed form for odd values of p using the generating function of the Legendre polynomials,

$$g(x,t) = \frac{1}{\sqrt{1-2xt+t^2}} = \sum_{i=1}^{\infty} t^i P_i(x). \tag{D.16}$$

By taking derivatives with respect to t we can pull down powers of i in the sum,

$$\sum_{i=0}^{\infty} \left(\prod_{k=1}^{n}(i+k)\right)^2 t^i P_i(x) = \left(\frac{\partial}{\partial t}\right)^n t^n \left(\frac{\partial}{\partial t}\right)^n t^n g(x,t) = g^{(n)}(x,t). \tag{D.17}$$

So for odd powers of p, with $p > 1$ we have a closed form for the mean power between two parallel cylindrical shells,

$$\mathcal{D}_p(a,b) = \frac{4\pi^{5/2}}{\Gamma\left(\frac{p}{2}\right)\Gamma\left(\frac{p-1}{2}\right)} g^{\left(\frac{p-3}{2}\right)}\left(\frac{a^2+b^2}{a^2-b^2}, a^2-b^2\right). \tag{D.18}$$

Explicitly for $p = 3$ we can write,

$$D_3(a,b) = \frac{8\pi^2}{\sqrt{(1+a+b)(1-a-b)(1+a-b)(1-a+b)}}, \tag{D.19}$$

which is the cylinder result seen in equation (6.10).

D.2.1 Solid Cylinders

To look at the interaction between solid cylinders we will define

$$\begin{aligned} \mathcal{D}_p^{S\delta}(a,b) &= \int_0^b r\mathrm{d}r \mathcal{D}_p(a,r), \\ \mathcal{D}_p^{SS}(a,b) &= \int_0^a r\mathrm{d}r \int_0^b r'\mathrm{d}r' \mathcal{D}_p(r,r'). \end{aligned} \tag{D.20}$$

In this case, it is slightly easier to integrate the power series. For the case of a solid cylinder with a cylindrical shell, the series gives

$$\mathcal{D}_p^{S\delta}(a,b) = \frac{2\pi^{5/2}}{\Gamma\left(\frac{p}{2}\right)\Gamma\left(\frac{p-1}{2}\right)} \sum_{i=0}^{\infty}\sum_{j=o}^{i} \frac{\Gamma\left(\frac{p-1}{2}+i\right)^2}{\left((i-j)!\right)^2 j!(j+1)^2} a^{2i-2j} b^{2j+2}, \tag{D.21}$$

$$= \frac{2\pi^{5/2}b^2}{\Gamma\left(\frac{p}{2}\right)\Gamma\left(\frac{p-1}{2}\right)} \sum_{i=0}^{\infty} \frac{\Gamma\left(\frac{p-1}{2}+i\right)^2}{i!(i+1)!} (a^2-b^2)^i P_i^{(1,0)}\left(\frac{a^2+b^2}{a^2-b^2}\right), \tag{D.22}$$

$$= \frac{2\pi^{5/2}b^2}{\Gamma\left(\frac{p}{2}\right)\Gamma\left(\frac{p-1}{2}\right)} g_{(1,0)}^{\left(\frac{p-3}{2}\right)}\left(a^2-b^2, \frac{a^2+b^2}{a^2-b^2}\right). \tag{D.23}$$

The j sum in equation (D.21) can be summed by,

$$\sum_{j=0}^{i} \binom{i}{j}\binom{i+1}{j+1} x^j = (1-x)^i P_i^{(1,0)}\left(\frac{1+x}{1-x}\right), \tag{D.24}$$

where $P_i^{\alpha,\beta}(x)$ are the Jacobi polynomials. The Jacobi polynomials are a more general set of orthogonal polynomials, first studied by C. G. J. Jacobi [76], and P. L. Tchebychef [77] (a much more tractable modern paper is by Richard Askey [78]). The generating function for the Jacobi polynomials is

$$g_{(\alpha,\beta)}(x,t) = \frac{2^{\alpha+\beta}\left(1+t+\sqrt{1-2xt+t^2}\right)^{-\beta}}{\sqrt{(1-2xt+t^2)}\left(1-t+\sqrt{1-2x+t^2}\right)^{\alpha}} = \sum_{i=0}^{\infty} t^i P_i^{(\alpha,\beta)}. \tag{D.25}$$

By taking the proper combination of derivatives, it is possible to reproduce the expression found in equation (D.22) and resum the entire series for a closed form expression, equation (D.23), where $g_{(\alpha,\beta)}^{(n)}$ is the generating function.

$$\sum_{i=0}^{\infty}\left(\prod_{k=1}^{n}(i+k)\right)\left(\prod_{k=2}^{n}(i+k)\right) t^i P_i^{(1,0)}(x) = \frac{1}{t}\left(\frac{\partial}{\partial t}\right)^{n-1} t^n \left(\frac{\partial}{\partial t}\right)^{n} t^n g_{(1,0)}(x,t) = g_{(1,0)}^{(n)}(x,t). \tag{D.26}$$

For two solid cylinders we can write the mean distance as

$$\mathcal{D}_p^{SS}(a,b) = \frac{\pi^{5/2}}{\Gamma\left(\frac{p}{2}\right)\Gamma\left(\frac{p-1}{2}\right)} \sum_{i=0}^{\infty}\sum_{j=o}^{i} \frac{\Gamma\left(\frac{p-1}{2}+i\right)^2}{(i-j+1)!(i-j)!j!(j+1)^2} a^{2i-2j+2}b^{2j+2}, \tag{D.27}$$

$$= \frac{\pi^{5/2}b^2}{\Gamma\left(\frac{p}{2}\right)\Gamma\left(\frac{p-1}{2}\right)} \sum_{i=0}^{\infty} \frac{\Gamma\left(\frac{p-1}{2}+i\right)^2}{i!(i+2)!} (a^2-b^2)^{i+1} P_{i+1}^{(1,-1)}\left(\frac{a^2+b^2}{a^2-b^2}\right), \tag{D.28}$$

$$= \frac{\pi^{5/2}b^2}{\Gamma\left(\frac{p}{2}\right)\Gamma\left(\frac{p-1}{2}\right)} g_{(1,-1)}^{\left(\frac{p-3}{2}\right)}\left(a^2-b^2, \frac{a^2+b^2}{a^2-b^2}\right). \tag{D.29}$$

The j sum can be carried using to get another Jacobi polynomial,

$$\sum_{j=0}^{i} \binom{i}{j}\binom{i+2}{j+1} x^j = (1-x)^{i+1} P_{i+1}^{(1,-1)}\left(\frac{1+x}{1-x}\right). \tag{D.30}$$

The i sum can be carried out by taking derivatives of the generating function,

$$\sum_{i=0}^{\infty}\left(\prod_{k=1}^{n}(i+k)\right)\left(\prod_{k=3}^{n}(i+k)\right) t^{i+1} P_{i+1}^{(1,-1)}(x) =$$

$$\sum_{i=0}^{\infty}\left(\prod_{k=0}^{n-1}(i+k)\right)\left(\prod_{k=2}^{n-1}(i+k)\right) t^{i} P_{i}^{(1,-1)}(x) =$$

$$\frac{1}{t^2}\left(\frac{\partial}{\partial t}\right)^{n-2} t^{n-1}\left(\frac{\partial}{\partial t}\right)^{n} t^{n-1} g_{(1,-1)}(x,t) = g_{(1,-1)}^{(n)}(x,t). \tag{D.31}$$